N-8044

AN EXPERIMENTAL INVESTIGATION OF THE EFFECTS OF TWO INLET-BOUNDARY-LAYER CONDITIONS ON THE PERFORMANCE OF A 12° CONICAL DIFFUSER OPERATING AT SUBSONIC MACH NUMBERS UP TO MACH NUMBER 1.0

A Thesis Presented to

The Faculty of the Department of Engineering

University of Virginia

In Partial Fulfillment

of the Requirements for the Degree

Master of Aeronautical Engineering

APR 1971
RECEIVED
NASA STI FACILITY
INPUT BRANCH

by

Barney Hugh Little, Jr.

April 1951

N71 72510
(ACCESSION NUMBER)
93
(PAGES)
TMX-67039
(NASA CR OR TMX OR AD NUMBER)
(THRU)
None
(CODE)
(CATEGORY)
FACILITY FORM 602

AN EXPERIMENTAL INVESTIGATION OF THE EFFECTS OF TWO INLET-BOUNDARY-LAYER CONDITIONS ON THE PERFORMANCE OF A 12° CONICAL DIFFUSER OPERATING AT SUBSONIC MACH NUMBERS UP TO MACH NUMBER 1.0

A THESIS PRESENTED TO
THE FACULTY OF THE DEPARTMENT OF ENGINEERING
UNIVERSITY OF VIRGINIA

IN PARTIAL FULFILLMENT
OF THE REQUIREMENTS FOR THE DEGREE
MASTER OF AERONAUTICAL ENGINEERING

By
BARNEY HUGH LITTLE, JR.

APRIL 1951

SUBMITTED IN PARTIAL FULFILLMENT OF THE REQUIREMENTS

FOR THE DEGREE MASTER OF AERONAUTICAL ENGINEERING AT

THE UNIVERSITY OF VIRGINIA

APRIL 30, 1951

AUTHOR Henry Hyde Tittle, Jr.

THESIS SUPERVISOR Kennedy J. Talbert

Clinton E. Brown

CHAIRMAN, COMMITTEE ON GRADUATE STUDIES IN ENGINEERING

Gordon K. Carter

ACKNOWLEDGEMENT

The assistance of Mr. Stafford W. Wilbur of the Internal Aerodynamics Section of the NACA at Langley Field, Va. is gratefully acknowledged. Mr. Wilbur assisted in measuring the data needed for this investigation and in preparing figures for the presentation of the results reported herein.

TABLE OF CONTENTS

CHAPTER		PAGE
I.	THE PROBLEM, DEFINITION OF TERMS USED, AND ORGANIZATION OF THE THESIS	1
	The Problem	1
	Statement of the Problem	1
	Importance of the Problem	2
	Definition of Terms Used	3
	Boundary-Layer Parameters	3
	Performance Parameters	5
	Symbols	7
	Organization of the Thesis	8
II.	REVIEW OF THE LITERATURE	9
	Individual Contributors	9
	Present Status of the Literature	10
III.	SOURCE OF THE DATA	12
	Apparatus	12
	Instrumentation	14
IV.	EXPERIMENTAL PROCEDURE	19
	Static-Pressure Distribution	19
	Mass Flow and Total-Pressure Loss Surveys	19
	Boundary-Layer Surveys	20
V.	COMPUTATIONAL METHODS	22
	Velocity Profiles	22
	Boundary-Layer Parameters	23
	Flow Rate Parameters	24
	Performance Parameters	24

CHAPTER PAGE

VI. RESULTS OF STATIC-PRESSURE DISTRIBUTION MEASUREMENTS AND DISCUSSION 27

Thinner-Inlet-Boundary-Layer Condition 27

Thicker-Inlet-Boundary-Layer Condition 29

Comparison of Thinner- and Thicker-Inlet-Boundary-Layer Conditions 29

Radial Static-Pressure Distributions 33

VII. RESULTS OF BOUNDARY-LAYER MEASUREMENTS AND DISCUSSION 36

Thinner Inlet Boundary Layer 36

Thicker Inlet Boundary Layer 53

Comparison of Boundary Layers in the Two Configurations 68

VIII. RESULTS OF PERFORMANCE MEASUREMENTS AND DISCUSSION 72

Loss Coefficient 72

Diffusion Factor 74

Pressure Efficiency 76

Diffuser Effectiveness 76

IX. SUMMARY AND CONCLUSIONS 80

Summary 80

Conclusions 81

BIBLIOGRAPHY 83

APPENDIX 85

LIST OF FIGURES

FIGURE		PAGE
1.	Line drawing of apparatus	13
2.	Thinner-inlet-boundary-layer configuration	15
3.	Thicker-inlet-boundary-layer configuration	16
4.	Boundary-layer rake	18
5.	Survey tube	18
6.	Variation of mean inlet Mach number and mean inlet Reynolds number with the pressure ratio $\frac{P_{ref}}{H_o}$	25
7.	Static-pressure distribution - thinner inlet boundary layer	28
8.	Static-pressure distribution - thicker inlet boundary layer	30
9.	Comparison of static-pressure distributions	31
10.	Radial static-pressure distribution - thinner inlet boundary layer	34
11.	Radial static-pressure distribution - thicker inlet boundary layer	35
12(a) to (g).	Boundary-layer profiles - thinner inlet boundary layer	37
13.	Variation of boundary-layer thickness with pressure ratio - thinner inlet boundary layer	44
14.	Variation of displacement thickness with pressure ratio - thinner inlet boundary layer	45
15.	Growth of displacement thickness in the thinner-inlet-boundary-layer diffuser	46
16.	Variation of momentum thickness with pressure ratio - thinner inlet boundary layer	47
17.	Growth of momentum thickness in the thinner-inlet-boundary-layer diffuser	48
18.	Variation of boundary-layer-shape parameter with pressure ratio - thinner inlet boundary layer	49

FIGURE PAGE

19. Growth of boundary-layer-shape parameter in the thinner-inlet-boundary-layer diffuser 50

20(a) to (g). Boundary-layer profiles - thicker inlet boundary layer 54

21. Variation of boundary-layer thickness with pressure ratio - thicker inlet boundary layer 61

22. Variation of displacement thickness with pressure ratio - thicker inlet boundary layer 62

23. Growth of displacement thickness in the thicker-inlet-boundary-layer diffuser 63

24. Variation of momentum thickness with pressure ratio - thicker inlet boundary layer 64

25. Growth of momentum thickness in the thicker-inlet-boundary-layer diffuser 65

26. Variation of boundary-layer-shape parameter with pressure ratio - thicker inlet boundary layer 66

27. Growth of boundary-layer-shape parameter in the thicker-inlet-boundary-layer diffuser 67

28. Comparison of nondimensional velocity profiles at boundary-layer station 1 70

29. Comparison of boundary-layer thickness parameters δ and δ^* in the diffuser 71

30. Variation of loss coefficient with pressure ratio 73

31. Variation of diffusion factor with pressure ratio 75

32. Variation of pressure efficiency with pressure ratio 77

33. Variation of diffuser effectiveness with pressure ratio ... 78

CHAPTER I

THE PROBLEM, DEFINITION OF TERMS USED, AND ORGANIZATION OF THE THESIS

The emphasis that has been placed, in recent years, on the use of jet-propulsion systems for aircraft has resulted in an urgent need for the better understanding of the internal aerodynamics of such systems - particularly at large Reynolds numbers and high subsonic Mach numbers. Many investigations of the basic components of such systems (expanding, converging, and straight-walled channels) have been made, but many of the data from these investigations are not applicable to present-day aircraft design because of Mach number and Reynolds number limitations. In order to meet this need, investigations of configurations comparable to those actually encountered in flight problems must be made.

I. THE PROBLEM

Statement of the problem. This investigation was designed to study the effect of inlet-boundary-layer conditions on the performance of a 12° 10-inch inlet-diameter diffuser. Since there is, at the present time, no satisfactory theory for predicting boundary-layer growth accurately in regions of severe pressure gradients where the rate of change of boundary-layer parameters is large, and since there is no theory at all for predicting boundary-layer development after separation has occurred, no theoretical analysis of the flow through this diffuser was attempted.

For the investigation two different boundary-layer conditions were set by using two lengths of constant-area inlet pipe ahead of the diffuser. The first section used was 9 inches long and the other was 68 inches long. The analysis was further broken down to study first, the effects of inlet boundary layer on the flow pattern through the diffuser and then the relation between various characteristics of the flow and the diffuser performance measured as the ratio of the actual rise in static pressure through the diffuser to that rise ideally possible. It was the design of this program to learn not only what the effects of inlet boundary layer are but also how these effects are brought about.

Inlet Mach number was varied from about 0.3 up to 1.0 by increasing the total pressure upstream of the diffuser. This process resulted in a variation of Reynolds number (based on inlet diameter) from about 1×10^6 to 4×10^6.

Importance of the problem. In many flow problems it is necessary to convert the kinetic energy of a high velocity airstream to static pressure energy at a lower velocity. This is accomplished in a subsonic flow by any type of geometric expansion of the flow channel. To operate without incurring high pressure losses, however, the expanding channel, or diffuser as it is usually called, must be of suitable configuration.

The diffuser is an important part of most jet-propulsion systems since at the normal operating velocities of aircraft using such systems air is of necessity inducted at a higher velocity and lower pressure than is desired at the engine inlet. The efficiency of the system is increased

by placing a diffuser downstream of the inlet so that as much compression as possible may take place ahead of the engine.

Diffusers are quite valuable in other applications also. The power required to operate wind tunnels is largely dependent on the pressure recovery downstream of the test section. The tunnel therefore operates with minimum power when the maximum diffusion is obtained.

These are only two of the more important ways that the diffuser is used in the aeronautical world. There are many other applications but these alone are sufficient to show the importance of a better understanding of diffuser flow.

The configuration chosen for this investigation was designed to study the effect of two important variables on a diffuser large enough to be compared with those used on aircraft. And the variables - flow rate and inlet-boundary-layer thickness - were also chosen so as to be comparable with the conditions to be encountered in flight. It is felt therefore that these data will help to fill an evident gap in the knowledge of internal flows.

II. DEFINITION OF TERMS USED

Boundary-layer parameters. Several parameters are commonly used in discussing boundary layers. They are boundary-layer thickness, δ, displacement thickness, δ^*, momentum thickness, θ, and shape parameter, $\frac{\delta^*}{\theta}$. Boundary-layer thickness is arbitrarily defined at the maximum distance from the wall at which retardation of the flow due

to the wall is observed. It is extremely difficult to pin-point this dimension exactly so that δ is generally defined as the distance from the wall at which the local velocity is some arbitrary percentage of the free-stream velocity. For this investigation, δ is defined as the distance from the wall at which the local velocity is equal to 0.95 times the free-stream velocity.

The displacement thickness, δ^*, is a quantitative measure of the flow deficiency created by the boundary layer. It is often visualized as the amount that streamlines are displaced from a surface by the presence of boundary layer. It is exactly defined as the height of boundary layer which when multiplied by a unit width and the free-stream velocity is equal to the difference between the quantity of mass that would flow through the boundary layer if all the air there were at free-stream velocity and the quantity of mass that actually flows through the boundary layer.

The momentum thickness, θ, is a quantitative measure of the momentum deficiency in the boundary layer. It is defined as the boundary-layer thickness that, when multiplied by a unit width and the product of the density and the square of the free-stream velocity, is equal to the difference in momentum that the boundary layer would have if it were all at free-stream velocity and the actual momentum of the boundary layer.

The shape parameter, $\frac{\delta^*}{\theta}$, is the ratio of displacement thickness to momentum thickness. Its value as a single parameter which defines boundary-layer shape is demonstrated in reference 1.

Performance parameters. Four parameters were used to present diffuser performance. These parameters were selected to show the contribution of various features of the flow to the over-all diffuser performance and also in order that these data might be easily compared with the data of other investigators.

The loss coefficient $\frac{\Delta H}{q_i}$ is the ratio of the mass weighted mean total pressure loss through the diffuser to the dynamic pressure at the inlet. This ratio is a convenient measure of pressure loss because it possesses the tendency to remain constant with varying density and flow rate as long as the flow pattern does not change.

The pressure efficiency $\frac{\Delta p}{\Delta q}$ is the ratio of static pressure rise through the diffuser to the decrease in dynamic pressure. This coefficient depends upon pressure losses due to friction or, in the case of supersonic flow, pressure losses due to shock waves. It can be expected to vary in a manner inverse to the variation of the loss coefficient.

The diffusion factor $\frac{\Delta q}{\Delta q_{ideal}}$ is the ratio of the actual decrease in dynamic pressure through the diffuser to that ideally possible. This ratio measures how much of the geometric expansion is utilized to convert impact pressure to static pressure. Anything such as thickening or separating boundary layer which reduces the effective area of the diffuser will reduce $\frac{\Delta q}{\Delta q_{ideal}}$.

An over-all measure of the ability of the diffuser to convert the entering dynamic pressure to static pressure at the exit is the ratio

of the actual static pressure increase through the diffuser to that ideally possible. This ratio $\frac{\Delta p}{\Delta p_{ideal}}$ is called diffuser effectiveness. It is also, since the ideal static pressure increase is equal to the ideal decrease in dynamic pressure, equal to the product of the pressure efficiency and the diffusion factor, $\frac{\Delta p}{\Delta p_{ideal}} = \frac{\Delta p}{\Delta q} \times \frac{\Delta q}{\Delta q_{ideal}}$.

SYMBOLS

p	static pressure
H	total pressure
ΔH	total-pressure loss through diffuser
Δp	static-pressure increase through diffuser
q	compressible dynamic pressure ($H - p$)
Δq	change in dynamic pressure through diffuser
u	local velocity within boundary layer
U	local velocity at edge of boundary layer
x	longitudinal distance along diffuser center line
y	perpendicular distance from diffuser wall
δ	boundary-layer thickness at 0.95 $\frac{u}{U}$, inches
δ'	boundary-layer thickness at 1.00 $\frac{u}{U}$, inches
δ^*	boundary-layer displacement thickness, inches
θ	boundary-layer momentum thickness, inches
$\frac{\delta^*}{\theta}$	boundary-layer-shape parameter
$\frac{\Delta H}{q_i}$	loss coefficient
$\frac{\Delta p}{\Delta q}$	pressure efficiency
$\frac{\Delta q}{\Delta q_{ideal}}$	diffusion factor
$\frac{\Delta p}{\Delta p_{ideal}}$	diffuser effectiveness

Subscripts:

o	reference stagnation conditions
i	diffuser inlet conditions
e	diffuser exit conditions

III. ORGANIZATION OF THE THESIS

In order that the reader may gain a comprehensive view of the organization of the thesis, a brief description of its division into chapters will be presented here. First the background of the problem and a summary of the present status of the literature is presented in the chapter "Review of the Literature."

The chapter "Source of the Data" describes the location of the experimental equipment, the power supply, and the instrumentation. The techniques applied in taking the data are then described in the chapter "Experimental Procedure." The final treatment of the data is then explained in the chapter "Computational Methods." In this chapter the assumptions necessary for the preparation of the data and the errors involved are described for each parameter used.

The results of the investigation are presented in three chapters dividing the analysis into a presentation of static pressure distributions, boundary-layer profiles and parameters, and performance parameters. These chapters also present a discussion of the results as related to previous investigations in diffusers and as interrelated one to another.

The final chapter summarizes the results of this investigation and presents a statement of the conclusions that may be drawn.

CHAPTER II

REVIEW OF THE LITERATURE

The subject of diffusers is one that has been widely explored. Much data are available for diffusers of all shapes and all sizes. The designer of today, however, is faced with a bewildering situation in attempting to apply these data to present-day problems. To understand why this is so it is necessary to examine critically and objectively the field of diffuser literature.

I. INDIVIDUAL CONTRIBUTORS

Among the better known investigations of diffusers, the work of Gibson (reference 2) in 1909 is outstanding. He investigated the pressure drop through a number of conical diffusers for water flow. No attempt was made, however, to control the inlet boundary layer - in fact no mention is made of its consideration as one of the variables for diffuser performance. The Reynolds numbers of these tests ranged only up to about 2×10^3 at velocities up to 23 feet per second.

Squire (reference 3) investigated the performance of diffusers for air flow with a constant inlet length, thereby maintaining the inlet-boundary-layer constant. The Reynolds numbers of these investigations was about 1×10^6 but the Mach number was only about 0.4.

The performance of straight walled conical diffusers with inner bodies up to Mach number 1.0 was investigated by Bohm and Koppe (reference 4). These data are presented considering the inlet boundary layer

as negligible and furthermore the diffuser diameter was so small that the maximum Reynolds number was only about 1.4×10^5.

Naumann (reference 5) also investigated the performance of low-angle conical diffusers at Mach numbers ranging up to 1.0, but the inlet boundary layer was held constant by using a constant length of inlet pipe of 1.2 diameters. Power limitations made the size of the configuration, and consequently the Reynolds numbers for the data, of necessity small.

The effects of varying inlet boundary layer on the performance of diffusers is presented by Peters (reference 6). These data are presented also for varying diffusion angles. The inlet boundary layer was varied by adding straight pipe ahead of the diffuser entrance in units varying from 6 to 64 inlet diameters long. Unfortunately, however, these data are obtained at low flow rates, reaching a maximum Reynolds number of 2×10^5 at a Mach number of approximately 0.12.

These examples represent the most productive investigations to be found in diffuser literature. A large portion of these and other results are summarized by Patterson in reference 7 and Henry in reference 8.

II. PRESENT STATUS OF THE LITERATURE

The present status of diffuser literature is revealed to be inadequate to furnish information for the proper design of high-speed subsonic diffusers. Investigations at Mach numbers approaching 1.0 have generally been made with very small diffusers and no attempt has been

made to separate the effect of inlet-boundary-layer conditions. Those investigations which concerned diffusers of sizes comparable to those used in aircraft conversely were generally limited by the available power to very low Mach numbers. In addition, the type of flow at the diffuser inlet is for the majority of the literature unknown, or else some easily defined condition such as fully developed turbulent pipe flow is set up. This latter condition is commonly found in the literature but in practice it is rarely met as a diffuser inlet condition.

There is indicated then a need for data in configurations comparable to those used in full-scale aircraft flying at velocities approaching the velocity of sound. There is also indicated a need of data for diffusers under varying inlet flow conditions. Literature covering a combination of these variables over the desired ranges is, at present, extremely limited.

CHAPTER III

SOURCE OF THE DATA

The source of the data is perhaps best described in two parts. The first part describes the apparatus in which the tests were run, their location, and the power supply. The second part describes the instrumentation used to collect the data.

I. APPARATUS

The experimental investigation reported here was conducted in the Internal Aerodynamics Section of the National Advisory Committee for Aeronautics at Langley Field, Va.

The air flow for this investigation was supplied by two 1000-horsepower centrifugal blowers in series which delivered 22,000 cubic feet per minute at approximately 1.4 atmospheres pressure at top speed. This air flow was channeled to the diffuser entrance bell through 54-inch-diameter ducting which served as a plenum chamber. Downstream of the diffuser this air was recirculated through the blowers. By means of this recirculation, the temperature of the air was raised enough to prevent condensation in the diffuser throat.

Several screens were placed approximately 12 feet upstream of the diffuser entrance bell to produce as uniform a flow as possible.

The diffuser, entrance bell, and inlet pipe were formed from 1/2-inch cold-rolled steel. This apparatus is shown in the line diagram of figure 1. The diffuser itself is constructed in two parts.

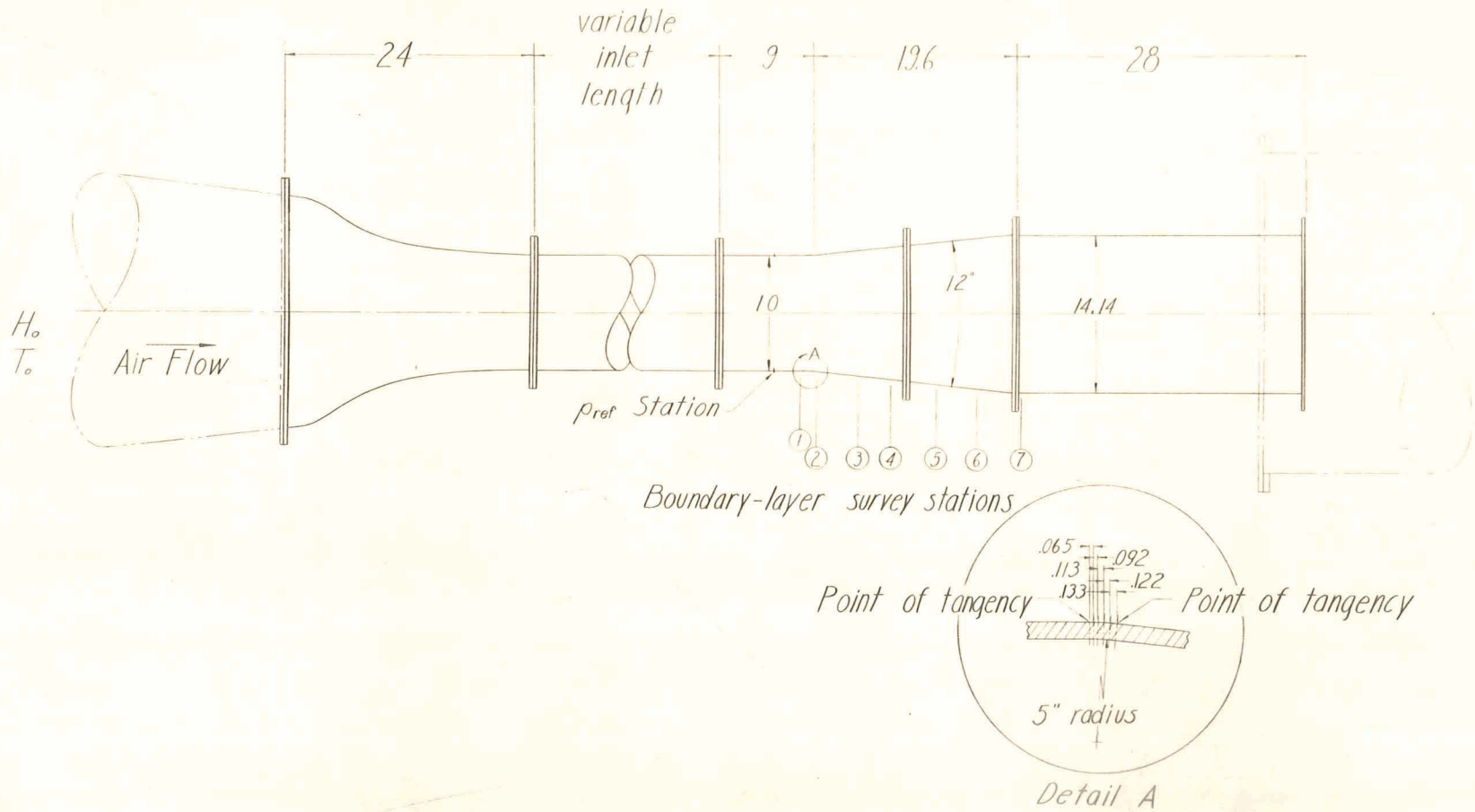

Figure 1. - Line drawing of apparatus.

The first part consists of a constant area inlet length of 9 inches leading to the diffuser, a transition region between the straight inlet and the conical diffuser section, and the first 9 inches of the diffuser. The other part is a truncated cone section 10.6 inches long, which completes the diffuser. The diffuser has a 10-inch-diameter inlet and 14.1-inch-diameter exit to give an exit-to-inlet area ratio of 2:1. The included conical angle is 12°. The inner surfaces of the entrance bell, the inlet length and the diffuser were machined, painted, and then finished with No. 600 "wet-or-dry" sandpaper. These parts were assembled and all joints were sealed with pyroxylin and sanded smooth.

For the thinner inlet-boundary-layer condition, only the 9 inches of inlet pipe integral with the diffuser was used. For the thicker inlet-boundary-layer condition, a 59-inch inlet section was added to make the total length of inlet section ahead of the diffuser 68 inches. A photograph of the short inlet configuration is shown in figure 2 and one of the long inlet configuration in figure 3.

II. INSTRUMENTATION

Stagnation temperature and pressure measurements were made in the 54-inch-diameter ducting upstream of the diffuser entrance bell. Temperature was measured with an iron-constantan thermocouple and potentiometer pyrometer, and total pressure was measured with a shielded total-pressure tube.

Static-pressure orifices were installed along a generatrix of the conical diffuser and in the inlet pipe at convenient increments of

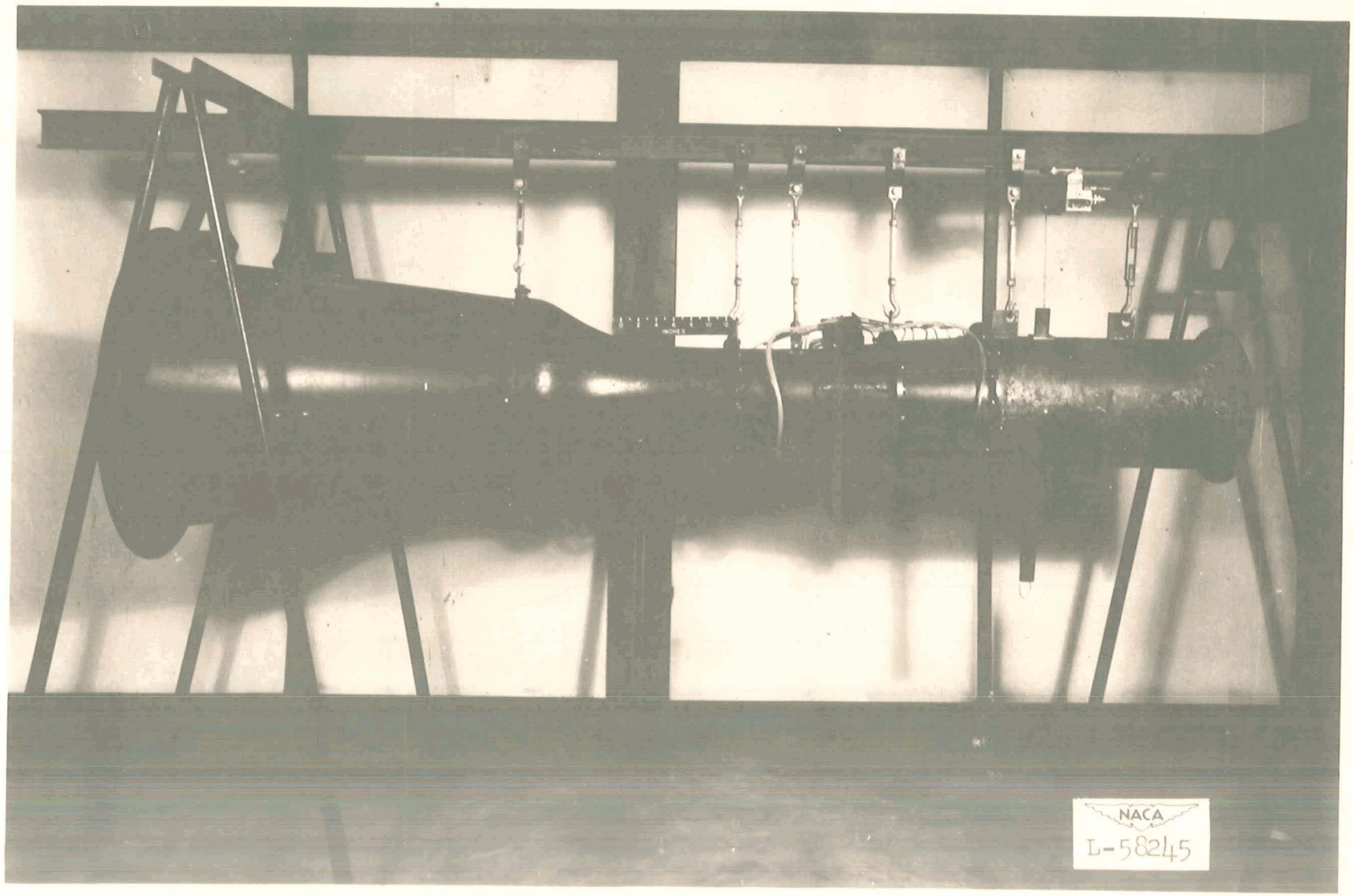

Figure 2.- Thinner-inlet-boundary-layer configuration.

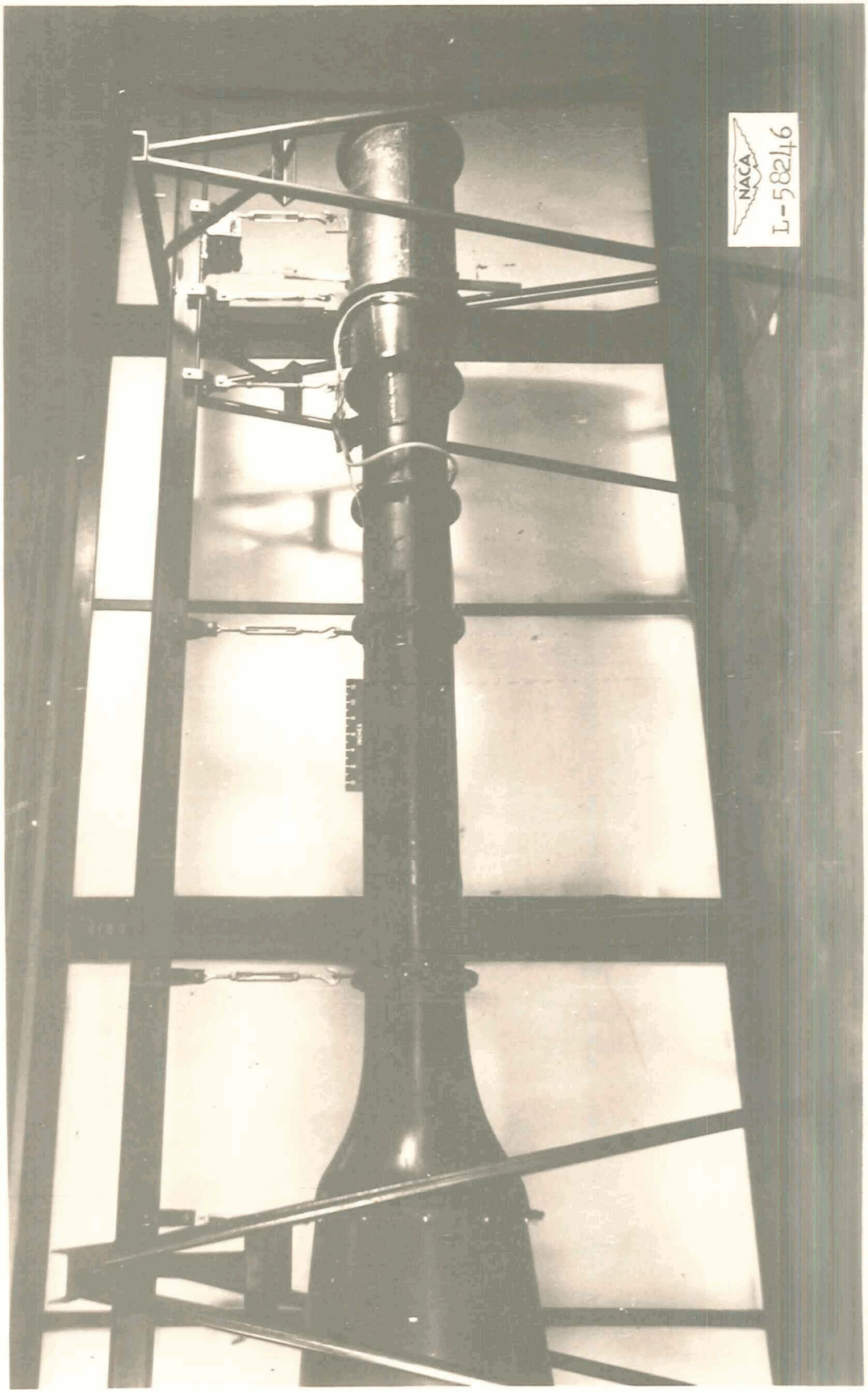

Figure 3. - Thicker-inlet-boundary-layer configuration.

distance. Six additional static-pressure orifices were equally spaced circumferentially around the ducting at the inlet and exit stations of the diffuser. In the transition region (see inset, figure 1) six static-pressure orifices were very closely spaced in order to measure accurately the abrupt pressure changes through this region. Since these orifices were located at such small longitudinal increments of distance it was necessary to stagger them circumferentially over a distance of about 1-1/2 inches.

Boundary-layer pressure surveys were made with the rake shown in figure 4. The tubes varied in size from 0.030-inch outside diameter for the tubes nearest the wall to 0.050-inch outside diameter farther out. A static-pressure tube was mounted on the rake to measure static pressures at the same longitudinal station as the total pressures were measured. In some cases near the diffuser exit the boundary layer was so thick that the rake did not entirely cover the distance to the edge of the boundary layer, and supplementary measurements were made with a movable pitot-static tube. This movable tube was designed to survey total and static pressures at the inlet and exit stations. As shown in figure 5 it was telescoped from 1/8-inch outside diameter at the upstream end to 5/8-inch outside diameter at the downstream end. In the tail pipe it was rigidly attached to a streamline strut which could be moved transversely to survey from wall to wall. By substituting tubes of various lengths it was possible to survey pressures at any station in the diffuser.

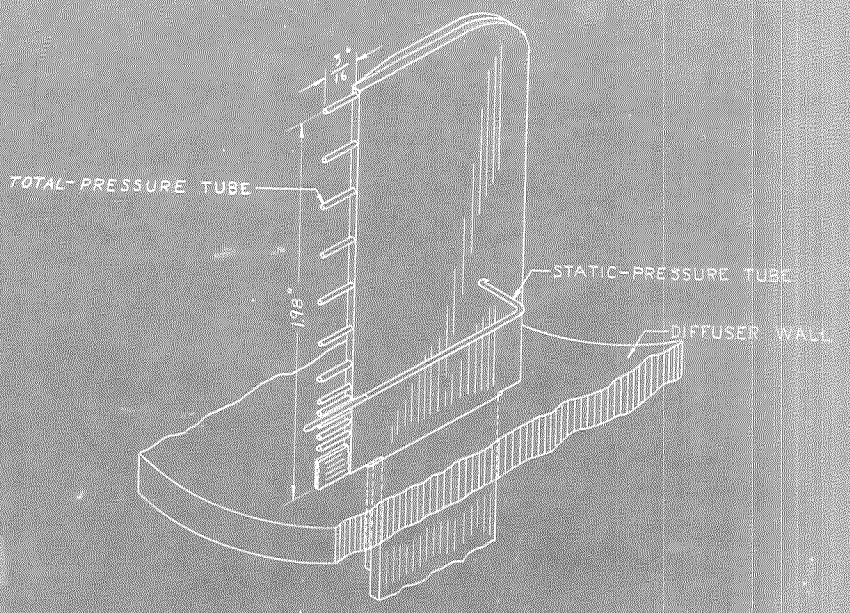

Figure 4.- Boundary-layer rake.

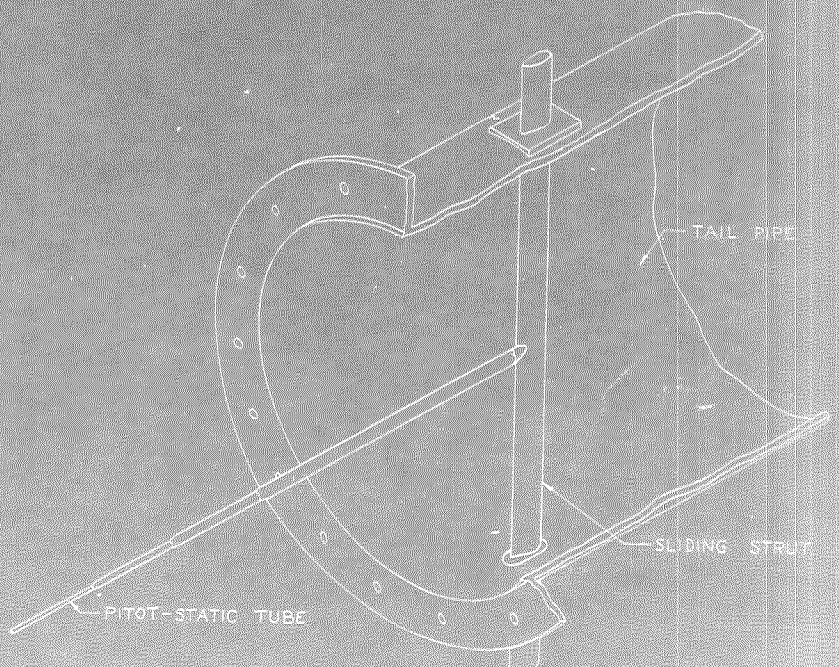

Figure 5.- Survey tube.

CHAPTER IV

EXPERIMENTAL PROCEDURE

In order that boundary-layer growth through the diffuser and performance might be thoroughly studied over the range of flows and inlet boundary layers discussed in Chapter I, it was necessary to survey the diffuser extensively. The methods used in making these experimental surveys will be described in this chapter.

I. STATIC-PRESSURE DISTRIBUTION

Before any boundary layer or mass flow data were collected, the static-pressure distributions through the inlet pipe and the diffuser were measured over the entire range of flow rates. The wall orifices described in Chapter III were connected to multitube manometers containing tetrabromoethane or mercury, as the case demanded, and at each flow rate the static-pressure distribution was photographically recorded.

II. MASS FLOW AND TOTAL-PRESSURE LOSS SURVEYS

Total- and static-pressure surveys were made at the diffuser inlet using the pitot-static tube shown in figure 5. This tube was moved diametrically from one wall to the duct center line as total- and static pressure were measured on multitube manometers. This process was carried out for a number of flow rates and a static-pressure orifice just upstream of the inlet (see figure 1) was read as a reference pressure for

each point. This survey was made as a calibration of the actual mass flow through the inlet against the reference pressure.

Another survey of total- and static pressure was carried out in the same manner at the pipe exit. From these surveys the mass weighted value of total pressure loss through the diffuser alone was obtained.

III. BOUNDARY-LAYER SURVEYS

The rake shown in figure 4 was installed at seven stations in the diffuser (see figure 1) to obtain knowledge of the growth of boundary layer. In order to install this rake it was necessary to cut holes in the diffuser wall. The rakes were then installed by removing the tail-pipe section. On the outside of the diffuser wall the rake was clamped securely, once its proper setting had been established, to a bracket attached to the diffuser wall with machine screws. The space where the rake entered the wall was then sealed with clay and masking tape. The rake surveys were begun at the diffuser exit and each installation hole was cut as the survey position was moved upstream. Each installation hole was carefully filled with pyroxylin after the rake was removed. The inner surface surrounding these holes was then carefully refinished with No. 600 "wet-or-dry" sandpaper. The pressure rakes were connected to multitube manometers and the entire boundary-layer survey was simultaneously made by photographing the manometer boards.

At some stations near the diffuser exit the pressure rake was not long enough to cover the complete boundary layer. When this condition

existed a pitot-static tube long enough to reach the desired point was made and attached to the movable strut used for the inlet and exit mass flow surveys. By this means it was possible to extend the pressure surveys at any station to the point where free-stream velocity was obtained.

CHAPTER V

COMPUTATIONAL METHODS

In some parts of the computation of data it was found that much time could be saved by making appropriate assumptions or short cuts at little expense in accuracy. In other cases it was found that parts of the data could be extended considerably if certain assumptions were made. In order that these assumptions might be clearly presented and that the meaning of all parts of the presented data be clearly understood, the methods of computation of the parameters and quantities used in this analysis will be described.

I. VELOCITY PROFILES

The ratio of the velocity inside the boundary layer to the velocity at the edge of the boundary layer was determined by the following formula:

$$\frac{u}{U} = \sqrt{\frac{H - p}{H_{max} - p}}$$

The value H_{max} is the maximum total pressure read at that station, and p is the value of static pressure from the one static tube on the boundary-layer survey rake. The validity of the assumption that static pressure is constant across the boundary layer will be shown when the results of the static-pressure distributions are discussed.

It was found that the error in values of shape parameter $\frac{\delta^*}{\theta}$ caused by using this incompressible formula was less than -5 percent up

to local Mach numbers of about 0.7. Beyond this point the error increased gradually up to about -20 percent at local $M = 1.0$. Since most of the data presented are in the range where local $M < 0.7$, the simplified incompressible formula was used throughout.

This assumption of constant density across the boundary layer was also used to compute the boundary-layer parameters δ^*, θ, and $\frac{\delta^*}{\theta}$. It was found that these incompressible values were adequate for comparison of profile shapes under the conditions of this investigation. This assumption also makes comparison with the data of other investigators easier since most of the available data are presented in the incompressible form.

II. BOUNDARY-LAYER PARAMETERS

The boundary-layer parameters, δ^* and θ, were computed for the separated-flow profiles as well as the unseparated-flow profiles. The graphical integration used to obtain δ^* and θ from these velocity profiles did not include the area bounded by the reversed-flow portion of the separated-flow profiles because the instrumentation used was not able to measure negative velocities. Therefore, the values of these parameters for the separated-flow profiles will be in error by some negative amount, depending on the severity of the separation.

All boundary-layer parameters were computed using two-dimensional formulas. The three-dimensional values are valuable only when used in connection with momentum and energy changes through the flow. The

two-dimensional values adequately describe the boundary-layer thickness and shape and are commonly used when such data are computed for comparitive purposes.

III. FLOW RATE PARAMETERS

The ratio of the inlet reference static pressure to the stagnation pressure $\frac{P_{ref}}{H_o}$ is used as a correlating parameter for the performance and boundary-layer curves. Decreasing values of $\frac{P_{ref}}{H_o}$ indicate increasing rate of flow. The position of the orifice used for p_{ref} is shown in figure 1. The parameter $\frac{P_{ref}}{H_o}$ is plotted against mean inlet Mach number and Reynolds number in figure 6.

IV. PERFORMANCE PARAMETERS

The total pressure losses through the diffuser were determined from mass weighted averages of pressure surveys at the inlet and exit by the method explained in reference 9. From these surveys were obtained $\overline{\frac{H_o - H_i}{H_o}}$ and $\overline{\frac{H_o - H_e}{H_o}}$, respectively. Then the total pressure loss was found as:

$$\frac{\Delta H}{H_o} = \overline{\frac{H_o - H_e}{H_o}} - \overline{\frac{H_o - H_i}{H_o}}$$

The change in static pressure through the diffuser was read from wall orifices around the inlet and exit sections and the change in dynamic pressure was then obtained as:

$$\frac{\Delta q}{H_o} = \frac{\Delta H}{H_o} - \frac{\Delta p}{H_o}$$

Figure 6. — Variation of mean inlet Mach number and mean inlet Reynolds number with the corresponding pressure ratio parameter.

The only other value needed to compute the performance is that of the ideal increase in static pressure through the diffuser. This was computed using the relations between mass flow and the ratio of static pressure to total pressure.

CHAPTER VI

RESULTS OF STATIC-PRESSURE DISTRIBUTION MEASUREMENTS AND DISCUSSION

In the work of von Doenhoff and Tetervin (reference 11) and numerous other investigators, it is pointed out that one of the primary variables controlling the development of a turbulent boundary layer is the existing pressure gradient. In any study of the boundary-layer action then it is important that the static-pressure distribution be known.

I. THINNER-INLET-BOUNDARY-LAYER CONDITION

The ratio of local static pressure to reference total pressure $\frac{P_{ref}}{H_o}$ is plotted against distance from the diffuser throat for different rates of flow in figure 7. It is shown that the static pressure decreases through the inlet bell, the straight inlet pipe, and in the first few inches downstream of the point where the walls begin to diverge. In the inlet pipe boundary-layer growth creates an effectively converging passage which accounts for the flow acceleration that causes the static-pressure decrease. Around the transition curvature joining the straight inlet pipe to the diffuser, the flow accelerates locally although the passage is expanding. This local acceleration around the relatively sharp corner creates a rather abrupt decrease in static pressure in the subsonic as well as the supersonic flows. In the cases where the local Mach number

Figure 7.- Static-pressure distribution through the boundary layer at various radial distances from diffuser inlet.

exceeds 1.0 (represented by all points where $\frac{p}{H} < 0.528$) the diverging passage acts as a supersonic nozzle and the flow continues to accelerate downstream of the transition curvature. In every case the pressure gradient becomes sharply positive downstream of this accelerated region, and the static pressure then continues to increase at a diminishing rate with increasing distance downstream. The intensity of the pressure gradients increases with increasing flow rate.

The pressure distribution through the thicker-inlet-boundary-layer configuration is shown in figure 8. At low flow rates the decreasing pressure through the long inlet pipe is not so obvious as it was in the thinner-inlet-boundary-layer case, but otherwise the pressure distributions are generally similar.

In order to point out more clearly the differences in pressure distributions in the two configurations, these distributions are plotted for several different flow rates in figure 9. To obtain the curves of figure 9 at the same values of $\frac{p_{ref}}{H_o}$ for each inlet-boundary-layer condition, the following procedure was used.

In the unchoked condition, a cross plot of figure 8 was obtained by plotting static pressure at each orifice against $\frac{p_{ref}}{H_o}$. Then for any value of $\frac{p_{ref}}{H_o}$ for which a pressure-distribution curve was available for the thinner-inlet-boundary-layer condition, a faired curve could be obtained for the thicker-inlet-boundary-layer condition. When the diffuser choked, however, a situation arose which made it impossible to continue this method of comparison. The thicker inlet boundary layer

Fig. 9 Pressure distribution from different methods, $M_{sd} = 0.96$, $\alpha = 3°$, $Re = 2.7 \times 10^6$

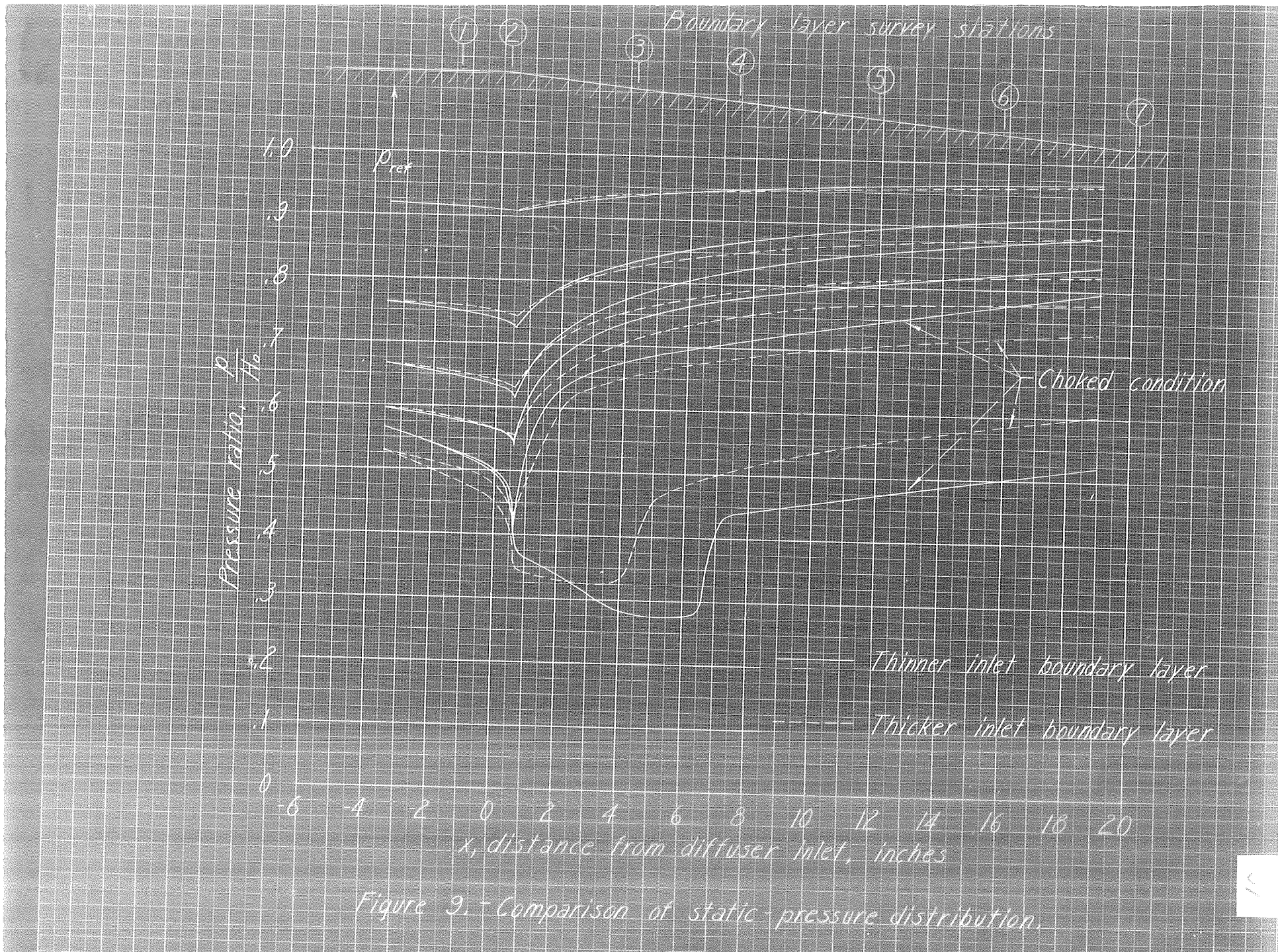

Figure 9. - Comparison of static-pressure distribution.

was affected by the negative pressure gradient existing in the transition region farther upstream than the thinner inlet boundary layer. For the thicker-inlet-boundary-layer case a thinning of the boundary layer occurred farther upstream in the inlet section. This process did two things: (1) It created an effective throat upstream of that found in the thinner-inlet-boundary-layer case, and (2) it increased the effective radius of curvature in the transition region. If the point where $\frac{p}{H_o} = 0.528$ $(M = 1.0)$ is considered to be the effective throat it can be seen in figure 9 that for the thicker-inlet-boundary-layer case the throat is displaced approximately 2 inches upstream of that for the thinner-inlet-boundary-layer case and approximately 3 inches upstream of the point where the transition region begins. Therefore, when the system was choked, the thicker-inlet-boundary-layer case attained values of $\frac{p_{ref}}{H_o}$ as low as 0.528, whereas the thinner-inlet-boundary-layer case could not attain values lower than $\frac{p_{ref}}{H_o} = 0.56$. This made it impossible to compare static-pressure-distribution curves from the two cases with equal values of $\frac{p_{ref}}{H_o}$ for the choked condition. Therefore, two arbitrary curves were selected from each case - one being the first choked point obtained, and the second being at the maximum-power-available condition.

It can be seen from figure 9 that in both configurations at subcritical flow rates (flow rates at which the local Mach number at every point is always less than 1.0) the point of minimum static pressure is located at $x = 0.60$ inch, which is about 0.10 inch downstream of the

point where the transition curvature ends.

In figure 9 it can be seen that the pressure gradients throughout the diffuser are not as great for the thicker inlet boundary layer as for the thinner inlet boundary layer. In the transition curvature region this is caused by the difference in effective radii of curvature created by the cushioning effect of the thicker boundary layer, and in the diffuser by the decreasing of effective expansion area created by the thicker boundary layer.

Radial distributions of static pressure, plotted as the ratio of absolute static pressure to reference stagnation pressure, at the inlet and exit stations are shown for the thinner inlet boundary layer in figure 10 and for the thicker inlet boundary layer in figure 11. Some radial surveys of static pressure (not shown) were also made at stations 5 and 6 for the thicker inlet boundary layer. At subcritical velocities the maximum variation of local static pressure from the value at midstream was less than ±3 percent. The first profiles to show a variation greater than 3 percent occurred at $\frac{p_{ref}}{H_o} \approx 0.57$. At the highest flow rates, however, variations as great as 30 percent were found.

It was also found that reference stagnation pressure existed at the diffuser center line in all cases except where shock losses occurred. For the subcritical flow rates, therefore, the values plotted of $\frac{p}{H_o}$ in figures 7 and 8 can be taken as the local midstream values of $\frac{p}{H}$ and the local Mach number obtained accordingly.

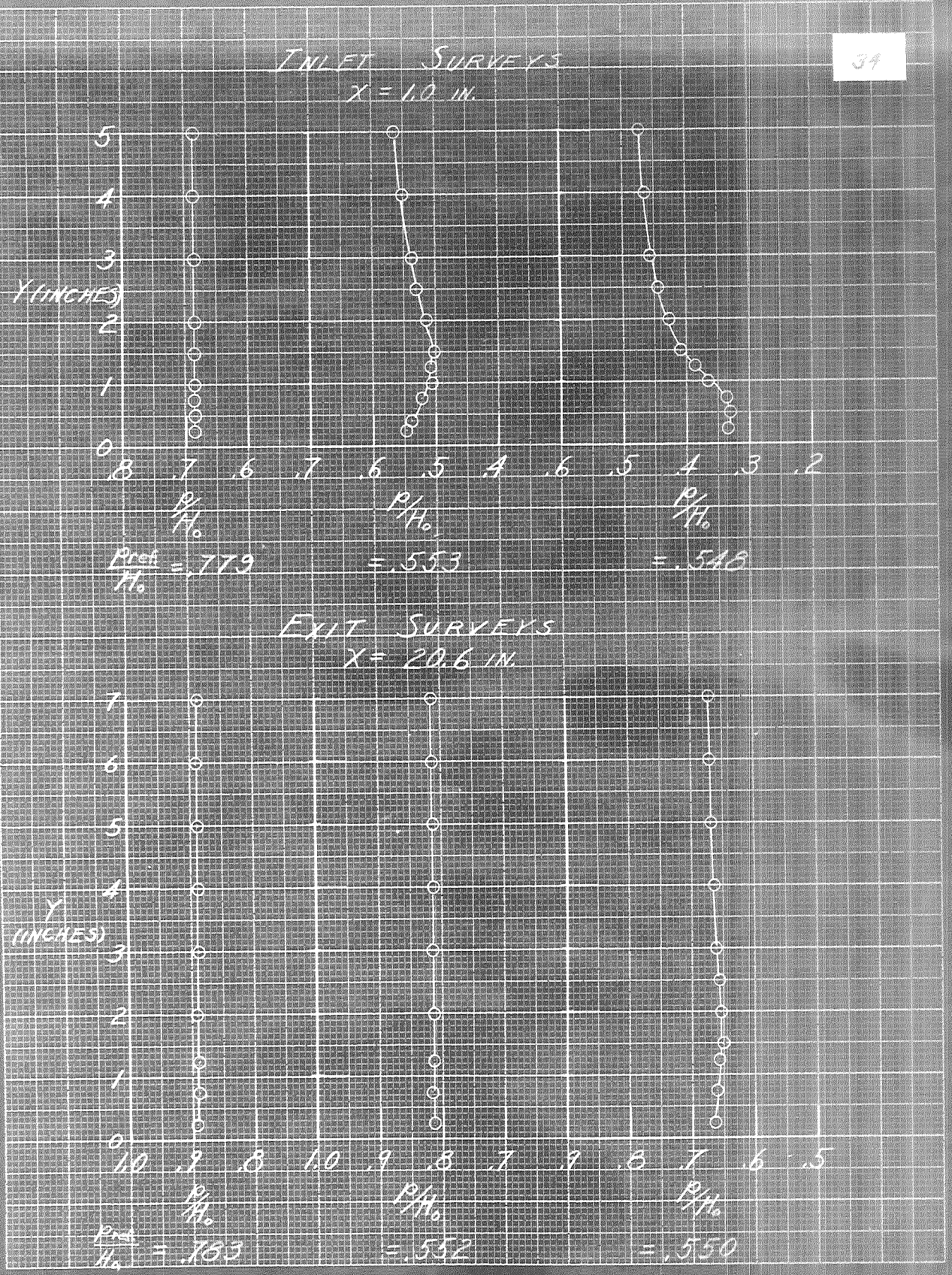

Figure 10. — Radial static-pressure distributions—thinner inlet boundary layer.

KEUFFEL & ESSER CO. MADE IN U.S.A.
NO. 334 — 2 TN. 10 X 10 TO THE HALF INCH.
100% RAG PAPER

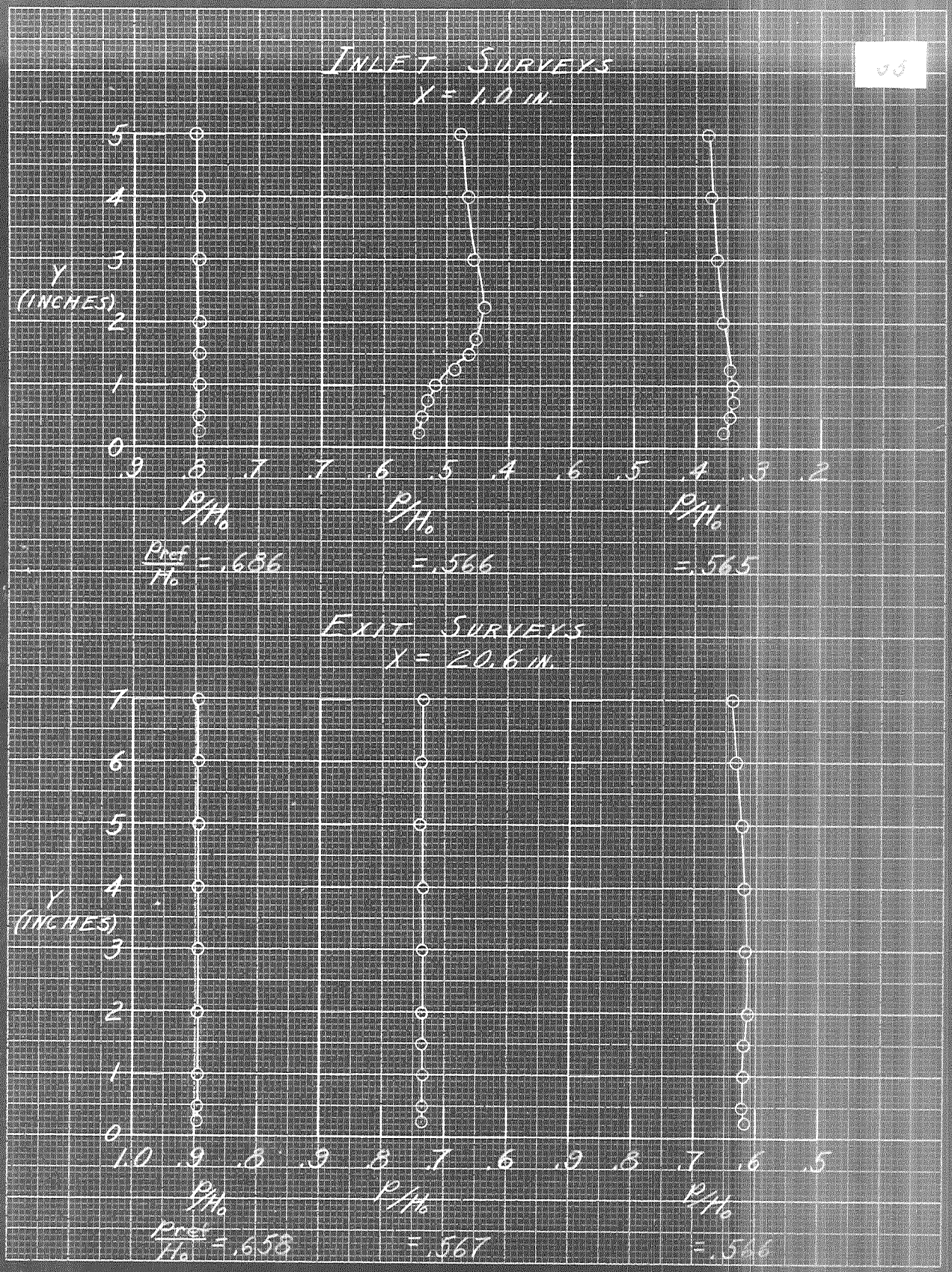

Figure 11. – Radial static pressure distributions – thicker inlet boundary layer.

KEUFFEL & ESSER CO. N.Y.

CHAPTER VII

RESULTS OF BOUNDARY-LAYER MEASUREMENTS AND DISCUSSION

The effective geometry of any duct system depends on the action of the boundary layer. Particularly is this true in a diffuser where the inherent positive pressure gradient can produce rapid changes in the boundary-layer thickness and in the resistance of the boundary-layer flow to separation from the boundary. It is important in an analysis of diffuser performance then that the action of the boundary layer be carefully examined.

I. THINNER INLET BOUNDARY LAYER

Representative boundary-layer velocity profiles at each survey station are plotted for the thinner inlet boundary layer in figures 12(a) to 12(g). The boundary-layer thickness, δ, is plotted against $\frac{p_{ref}}{H_o}$ in figure 13; δ^* is plotted against $\frac{p_{ref}}{H_o}$ in figure 14 and against x in figure 15; θ is plotted against $\frac{p_{ref}}{H_o}$ in figure 16 and against x in figure 17; and $\frac{\delta^*}{\theta}$ is plotted against $\frac{p_{ref}}{H_o}$ in figure 18 and against x in figure 19.

In some cases certain deficiencies in the data exist which require some explanation prior to an analysis of these figures. Near the diffuser exit (see fig. 12(f)) the data taken were incomplete in that the boundary-layer thickness was greater than the 2-inch span of the boundary-layer survey rake. In these cases it was believed that the

Figure 12. - Boundary layer profiles - thinner inlet boundary layer.
(a) Station 1.

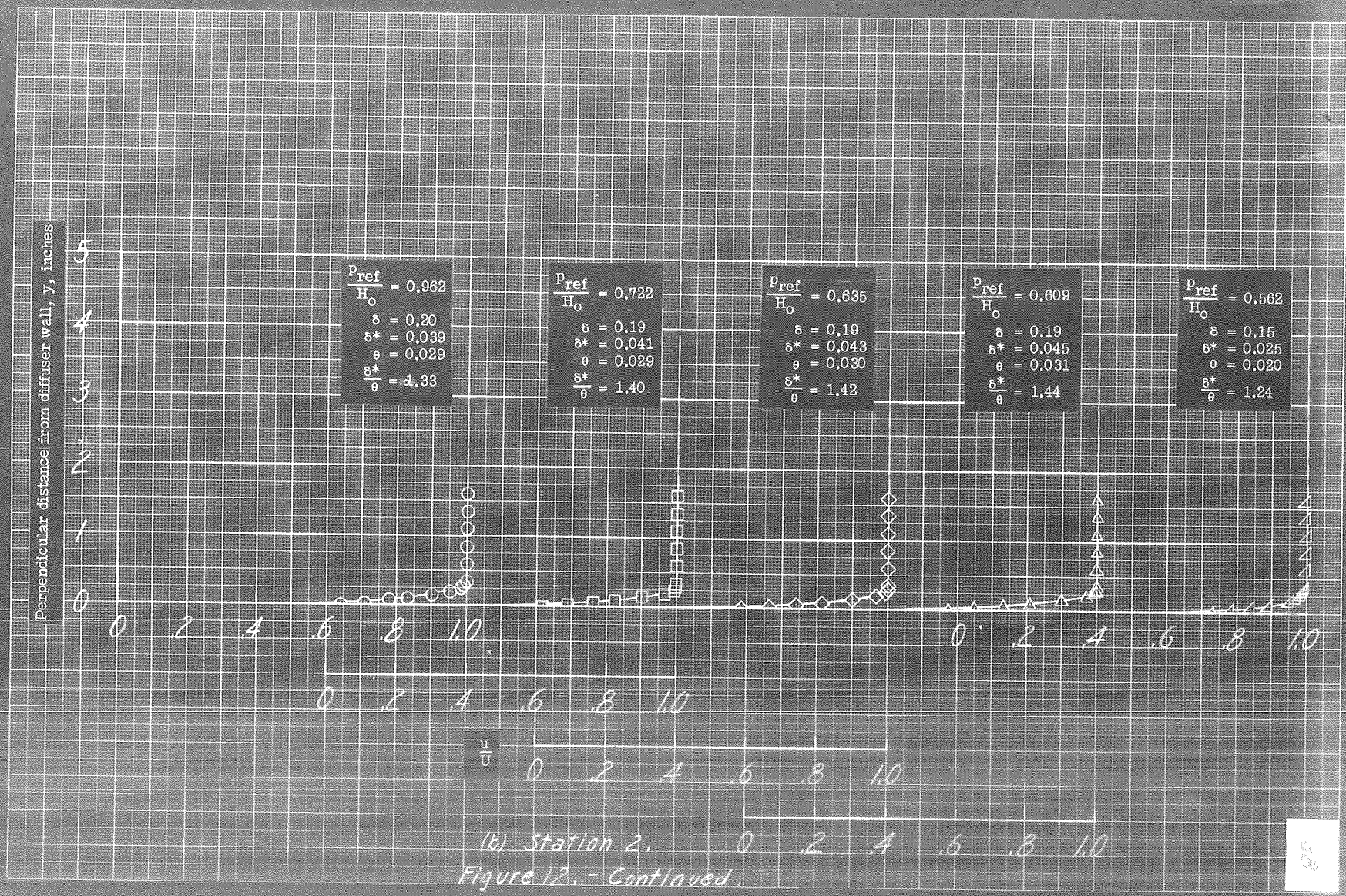

(b) Station 2.

Figure 12. - Continued.

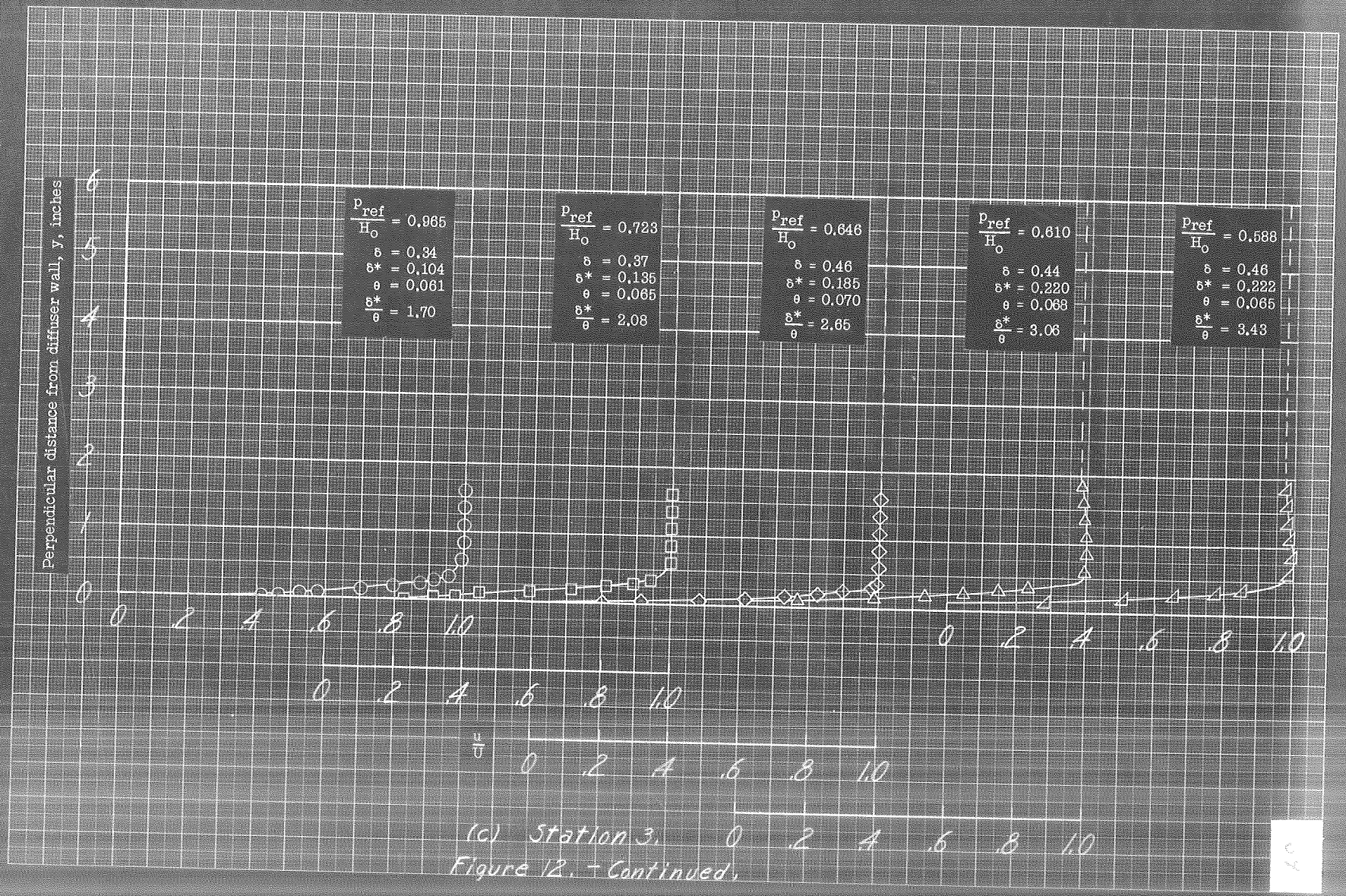

(c) Station 3.

Figure 12. - Continued.

(d) Station 4.

Figure 12. - Continued.

(e) Station 5.

Figure 12. - Continued

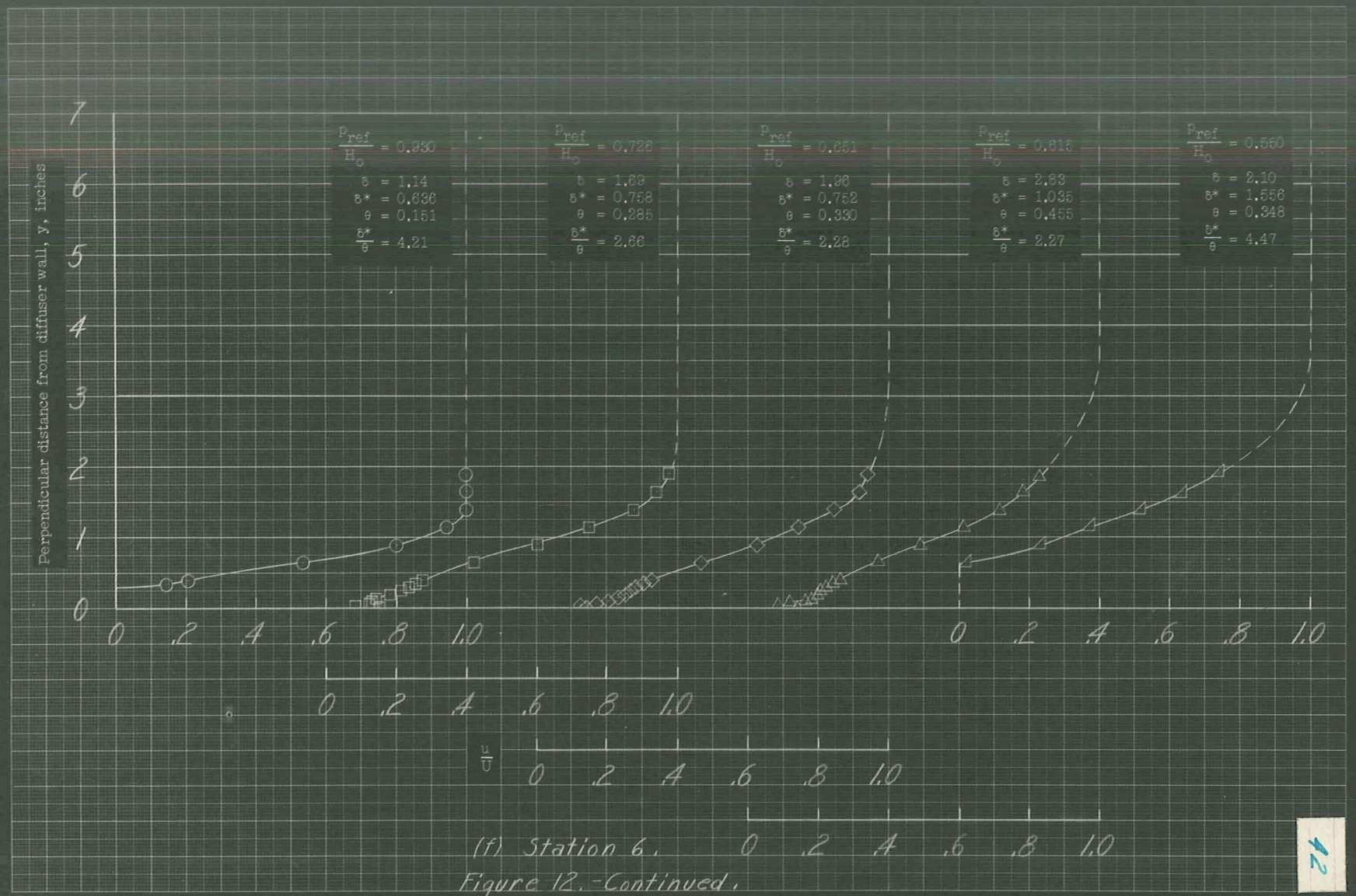

(f) Station 6.

Figure 12.-Continued.

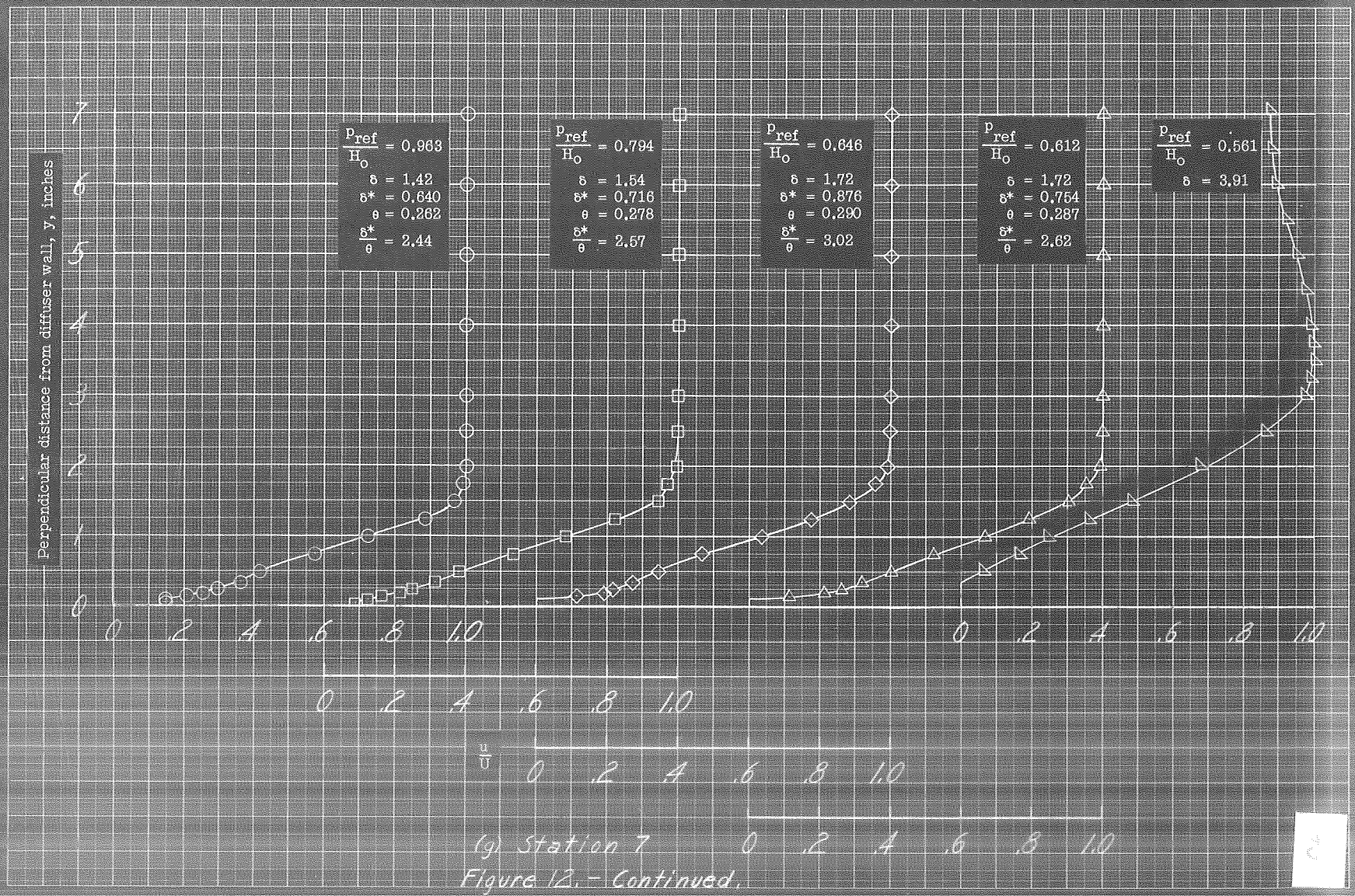

(g) Station 7

Figure 12. – Continued.

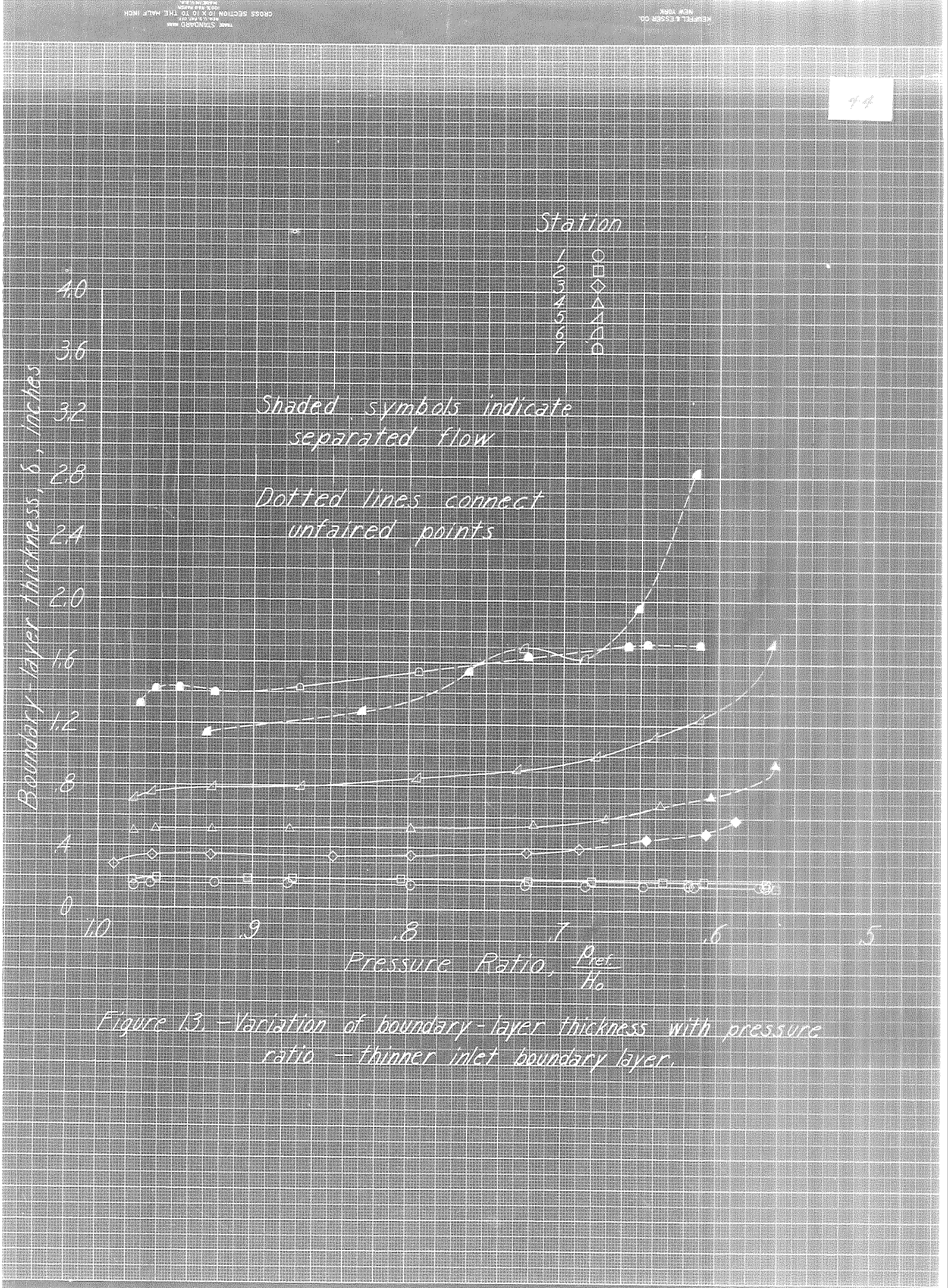

Figure 13.—Variation of boundary-layer thickness with pressure ratio.—thinner inlet boundary layer.

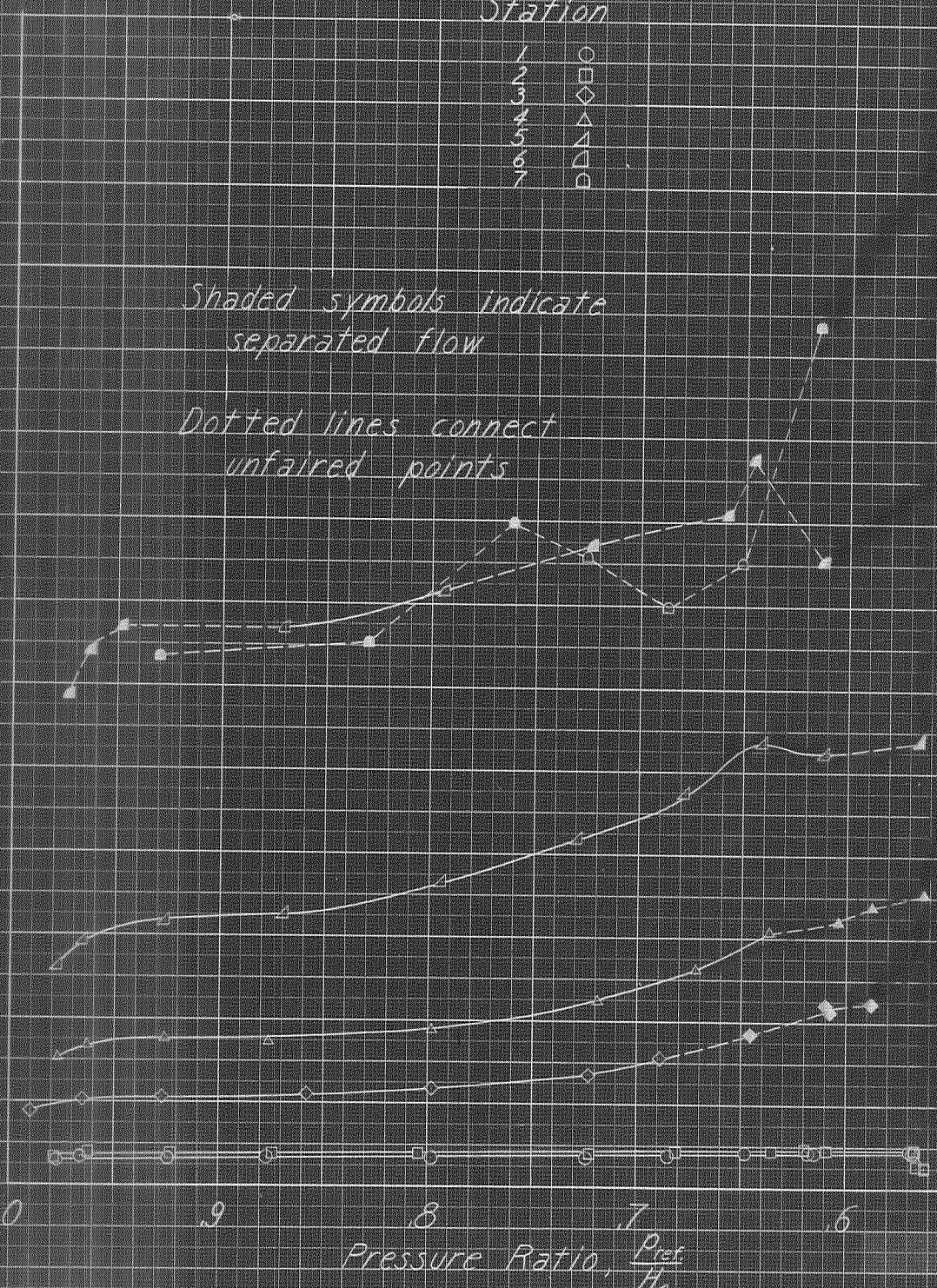

Figure 14. – Variation of displacement thickness with pressure ratio – thinner inlet boundary layer.

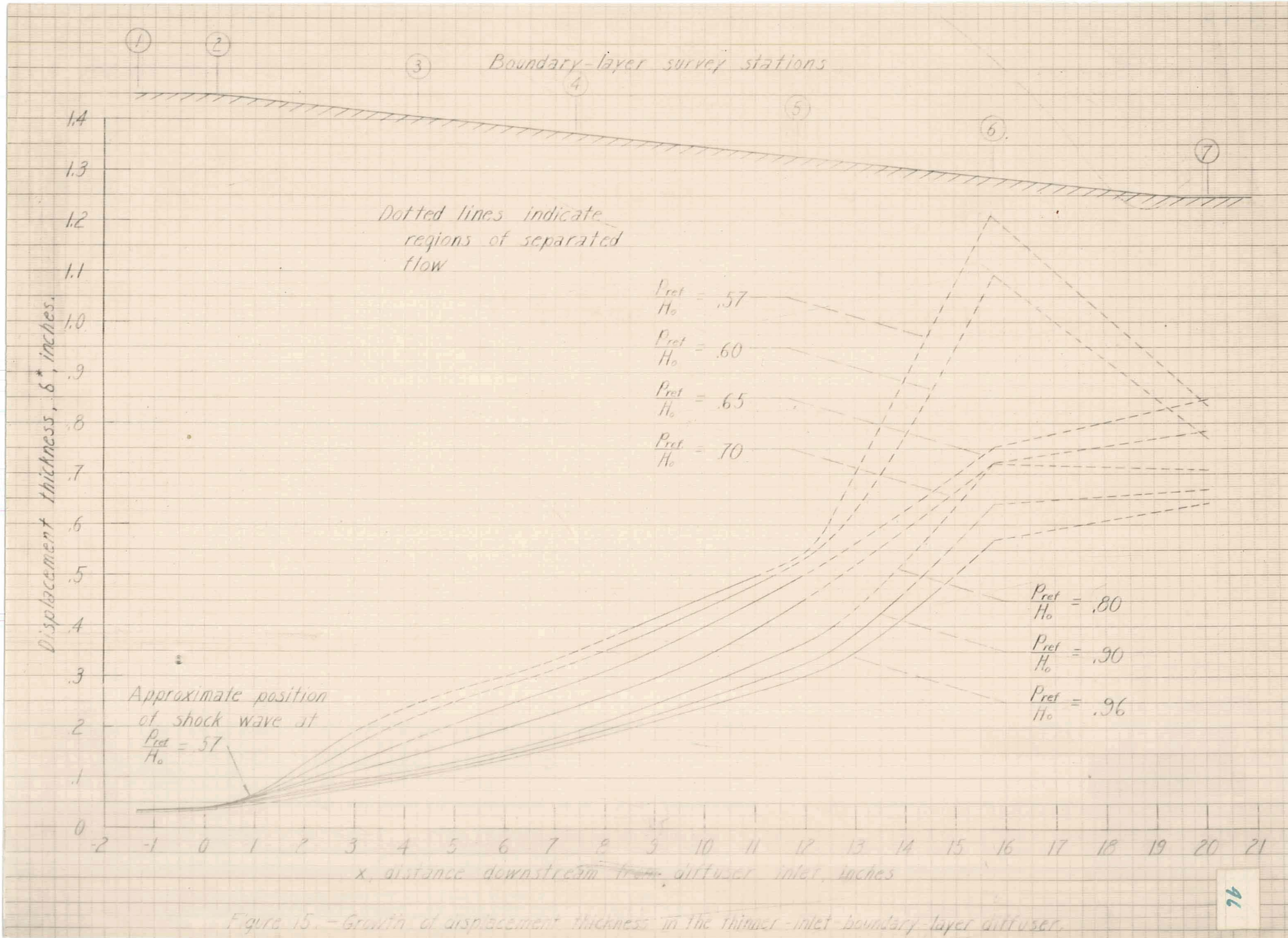

Figure 15.- Growth of displacement thickness in the thinner-inlet boundary-layer diffuser.

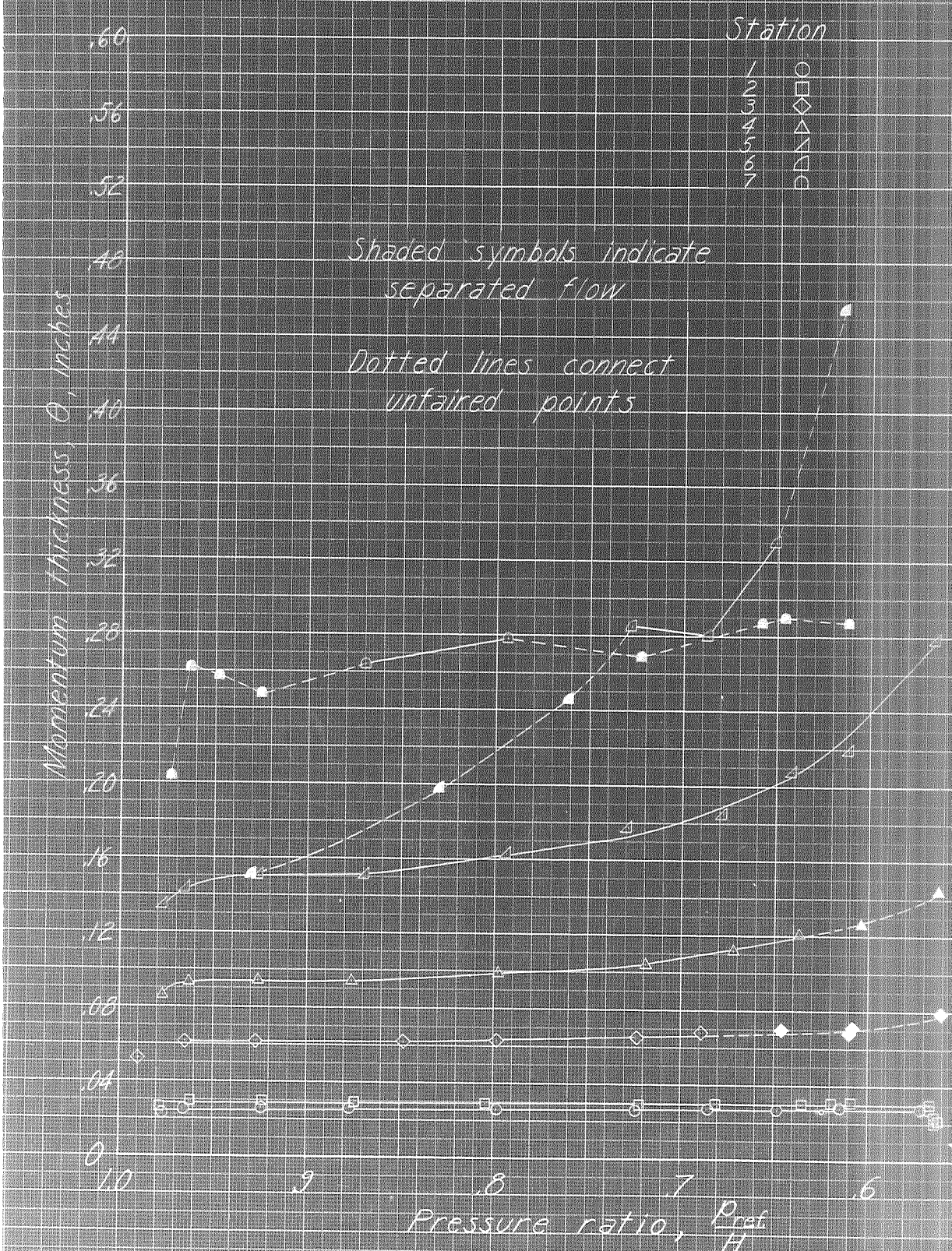

Figure 16.—Variation of momentum thickness with pressure ratio—thinner inlet boundary layer.

KEUFFEL & ESSER CO.
THIN STANDARD

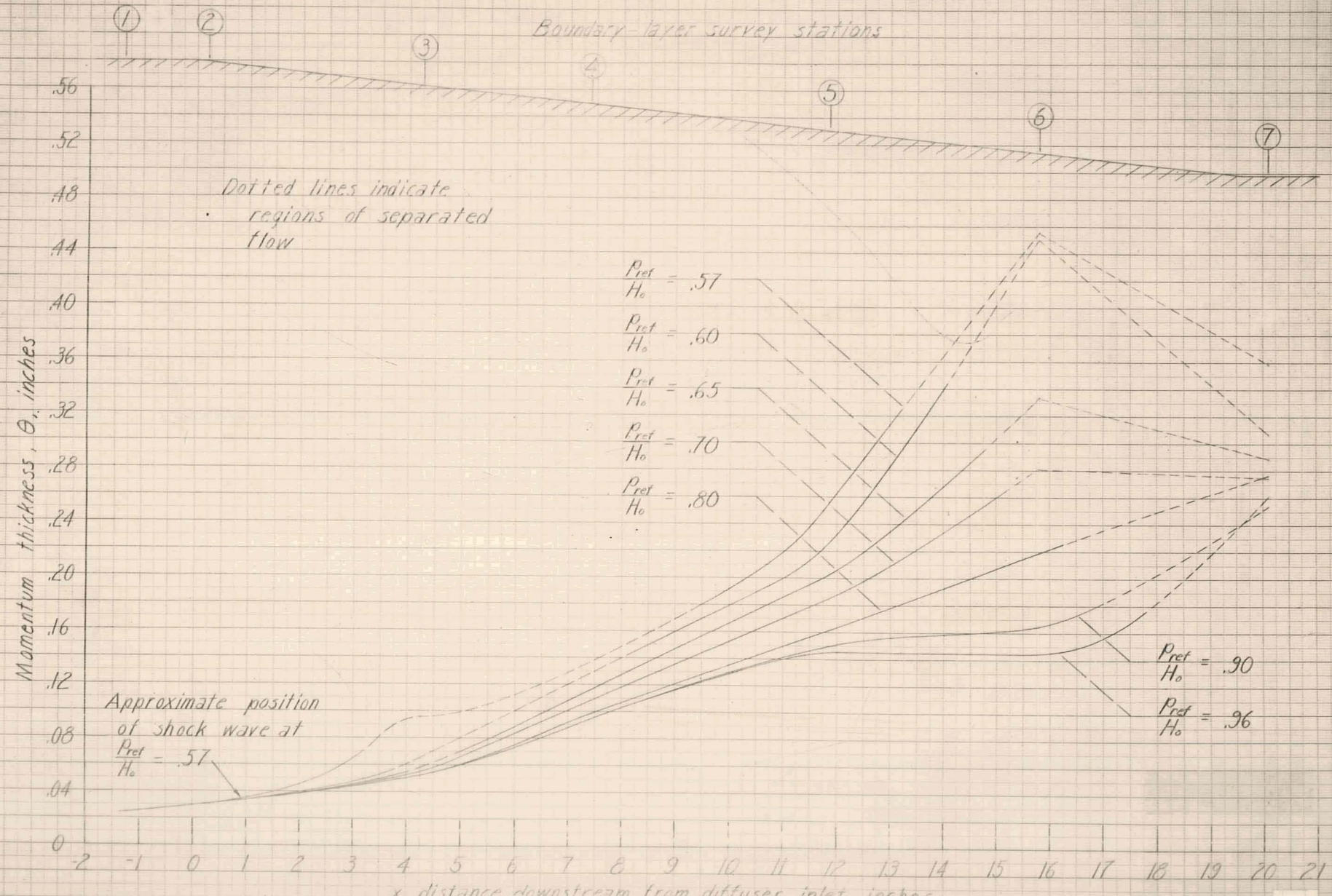

Figure 17. - Growth of momentum thickness in the thinner-inlet-boundary-layer diffuser.

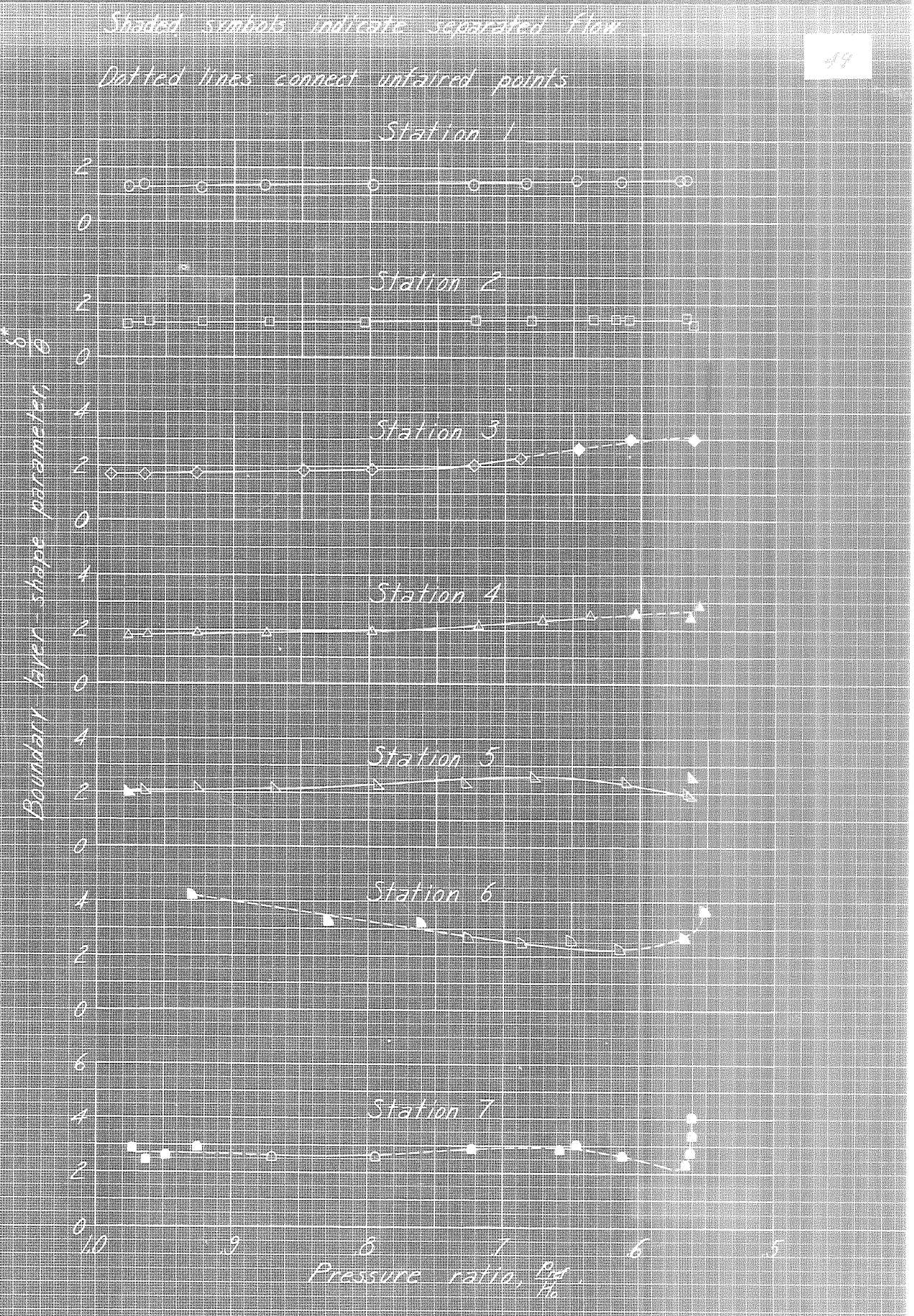

Figure 18 - Variation of boundary-layer-shape parameter with pressure ratio - thinner inlet boundary layer.

KEUFFEL & ESSER CO.
THIN STANDARD MINK
NEW YORK
CROSS SECTION MILLIMETER

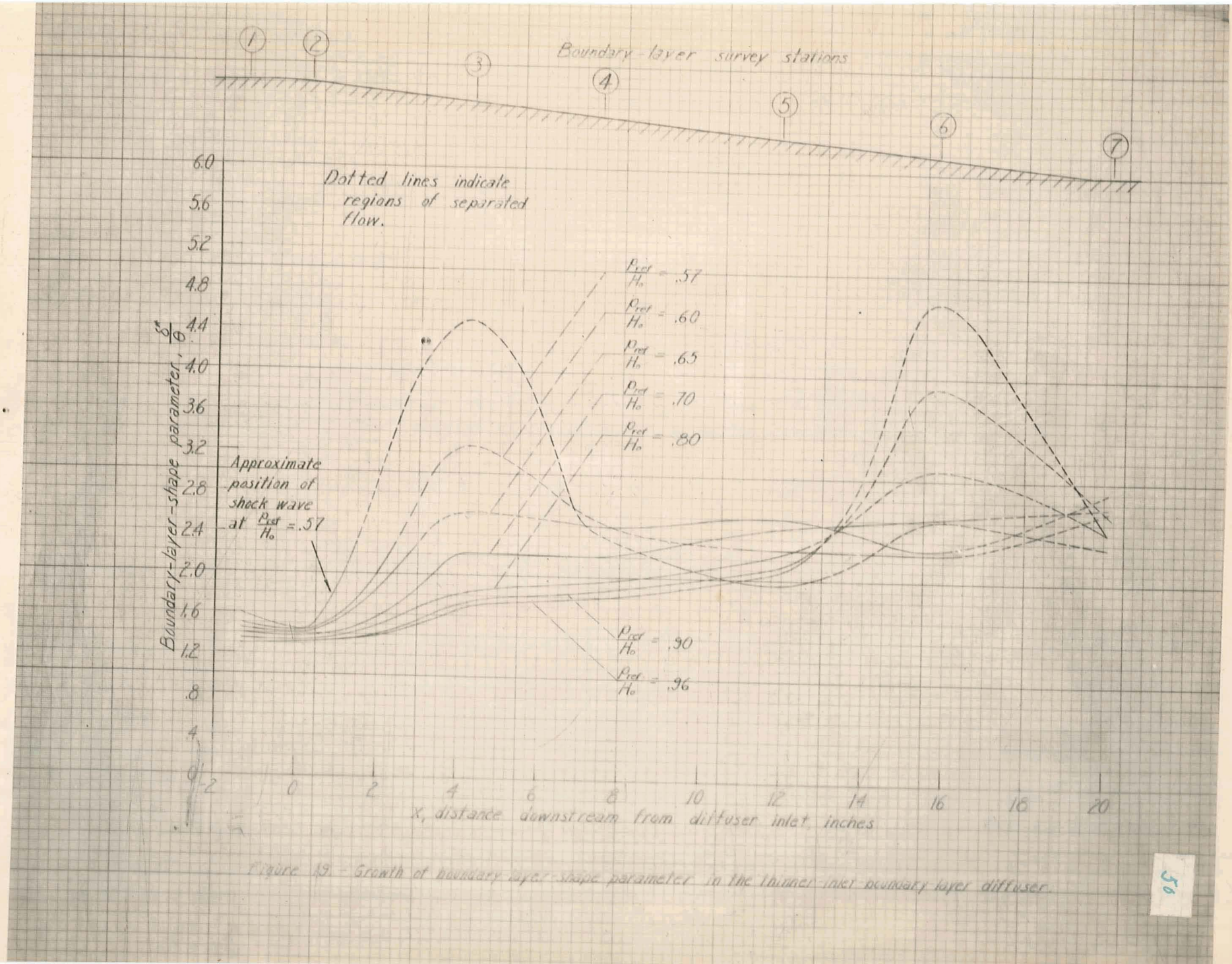

Figure 19 - Growth of boundary layer shape parameter in the thinner inlet boundary layer diffuser.

velocity distributions within the rake's span were of enough significance to present the data using H_o as the value of total pressure at the edge of the boundary layer. When this was done, solid lines were used to connect only the actual data points, and broken lines were used to represent the fairing of the profile to the midstream velocity as computed from the H_o values.

At the high flow rates where supersonic flow existed near the diffuser inlet, total-pressure surveys downstream of this region showed a deficiency from the reference value which was caused by shock losses. An extreme example of this is shown for $\frac{p_{ref}}{H_o} = 0.561$ in figure 12(g). In these cases it is impossible to determine at what point the boundary-layer pressure loss ends, so U was computed at the point where the maximum total pressure was measured. No attempt was made to determine δ^* or θ except in those cases where the maximum total pressure was equal to H_o.

For the separated profiles (in the present discussion, a separated profile is arbitrarily defined as one in which the point $\frac{u}{U} = 0$ is displaced a measurable distance from the wall) some significance of the boundary-layer parameters is lost, particularly in the case of $\frac{\delta^*}{\theta}$, for the single-parameter representation (reference 11) is no longer applicable. These parameters do retain some value, however, for comparative purposes and therefore are presented. All points on the boundary-layer curves that were obtained from separated profiles are indicated in each figure. No attempt is made to fair curves through these points.

They are connected with dotted lines and are presented merely to show the points at which separation was observed.

At subsonic inlet velocities where $\frac{P_{ref}}{H_o} > 0.65$, the flow pattern appears as a well-established flow except near the diffuser exit. At station 5 one separated profile was observed at the lowest flow rates. At stations 6 and 7, however, the flow pattern is very unstable and appears to follow no definite trends throughout the flow range. When the inlet velocity approached the point where local sonic velocity is attained in the transition curvature, separated profiles were observed at station 3, but the flow was reattached at station 5. When supersonic velocities were attained, all the profiles downstream of the shock terminating the supersonic region were separated.

As shown in figure 13, δ remains practically invariant at stations 1 and 2 with increasing velocity. In the diffuser itself, however, δ varies directly as a function of distance downstream from the inlet and inlet velocity. Figures 14, 15, 16, and 17 show that δ^* and θ vary in a manner similar to that of δ.

From the plots of figure 16 it appears that it is impossible to fix a value of $\frac{\delta^*}{\theta}$ where separation will occur. In agreement with the findings of reference 11, however, separated profiles were not observed at $\frac{\delta^*}{\theta} < 1.8$, nor attached profiles at $\frac{\delta^*}{\theta} > 2.6$ except for one or two isolated cases. Figure 19 provides a good picture of the regions in the diffuser where separation troubles occur for any flow rate. In general, at low flow rates, separation trouble begins near the diffuser exit, and at high flow rates near the diffuser inlet.

II. THICKER INLET BOUNDARY LAYER

Boundary-layer profiles in the diffuser are plotted for the thicker-inlet-boundary-layer condition in figure 20. At the extreme low flow rates, separation occurred at stations 5, 6, and 7. Through most of the subsonic-flow range, however, the flow remained attached throughout the diffuser. At station 3 at $\frac{p_{ref}}{H_o} < 0.65$, a small region of separated flow was observed. The flow was reattached at station 4. At supercritical velocities, shock-produced separation occurred as in the case of the thinner inlet boundary layer. An explanation of the types of profiles shown in figure 21 can be found in the explanation of the thinner-inlet-boundary-layer profiles on pages 33 and 48.

Boundary-layer thickness δ is plotted against $\frac{p_{ref}}{H_o}$ in figure 21. At stations 1 and 2, in the region of favorable pressure gradient, δ decreases with increasing flow rate but in the diffuser δ increases with increasing flow rate and distance from the inlet. The plots of δ^* against $\frac{p_{ref}}{H_o}$ in figure 22, δ^* against x in figure 23, θ against $\frac{p_{ref}}{H_o}$ in figure 24, and θ against x in figure 25 show about the same type variation as δ except at the lowest flow rates where the separated flow occurs.

Figures 26 and 27, in which the shape factor $\frac{\delta^*}{\theta}$ is plotted against $\frac{p_{ref}}{H_o}$ and x, respectively, show that the thicker inlet boundary layer is more stable than the thinner inlet boundary layer (see fig. 19) except at the lowest flow rates. At high-subsonic flow rates $\frac{p_{ref}}{H_o} \leq 0.7$ there is the same region of separated flow at station 3 that was observed for the thinner inlet boundary layer, but the flow appears to have re-established its normal pattern at station 5.

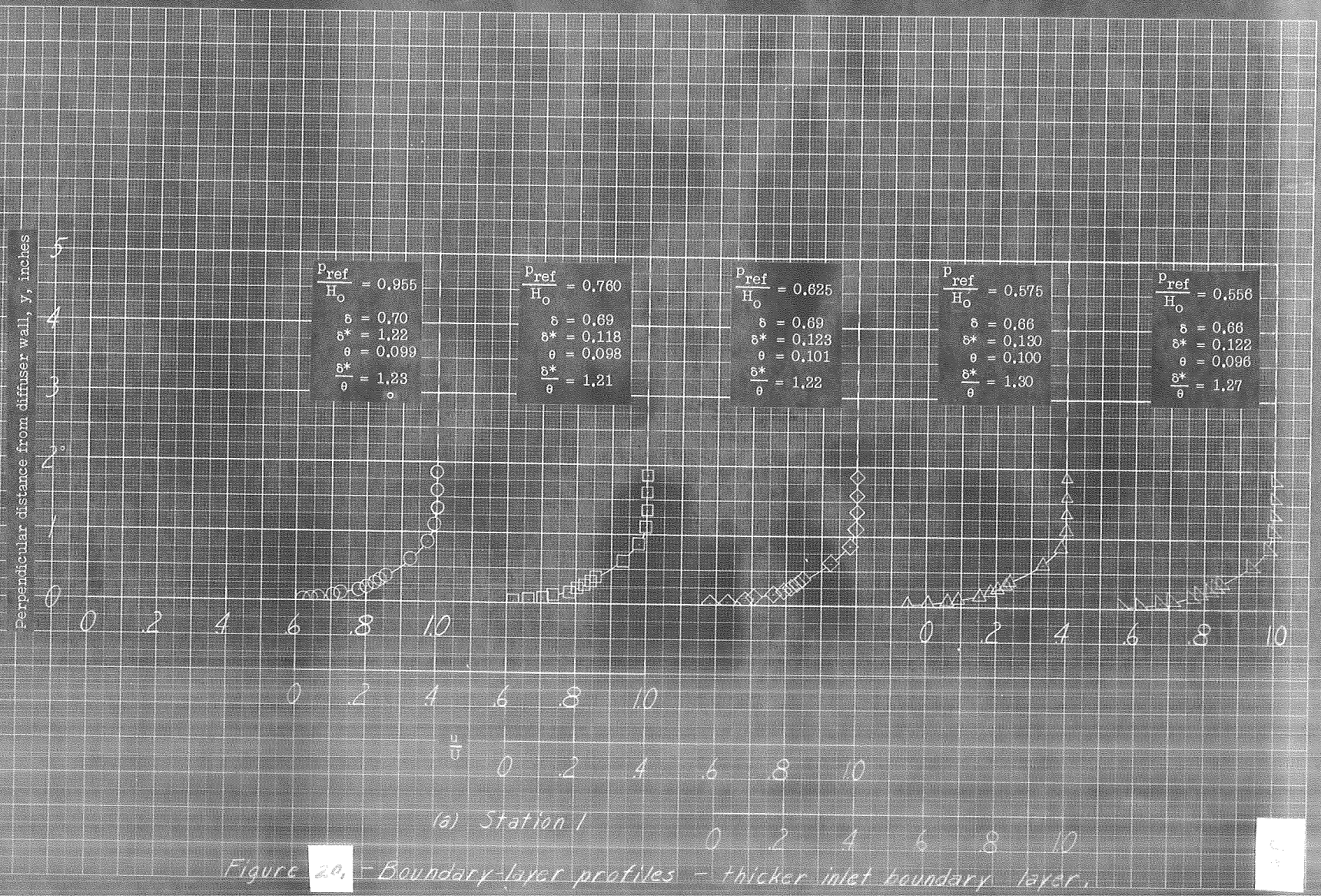

(a) Station 1

Figure 28. - Boundary-layer profiles - thicker inlet boundary layer.

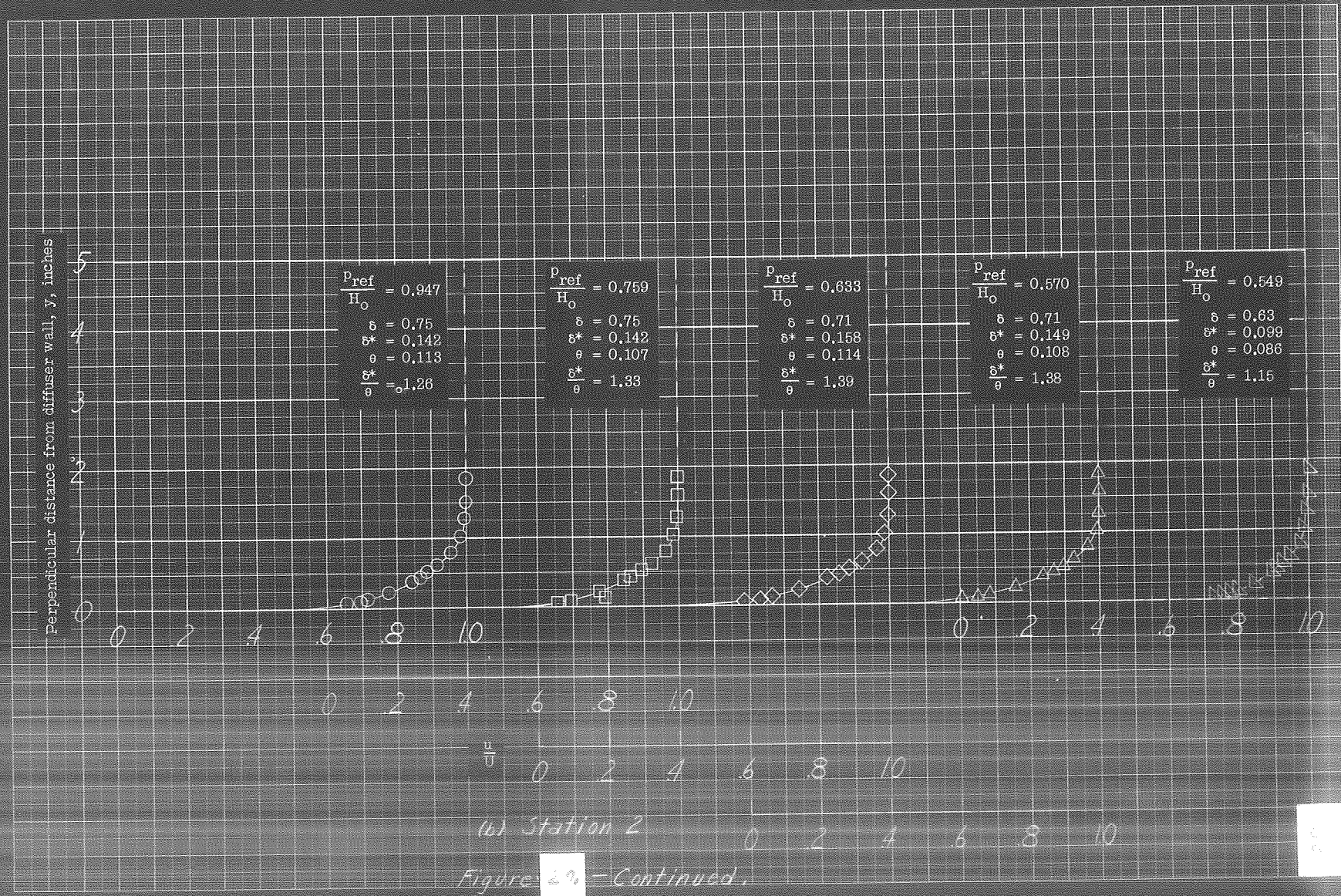

(b) Station 2

Figure 20.—Continued.

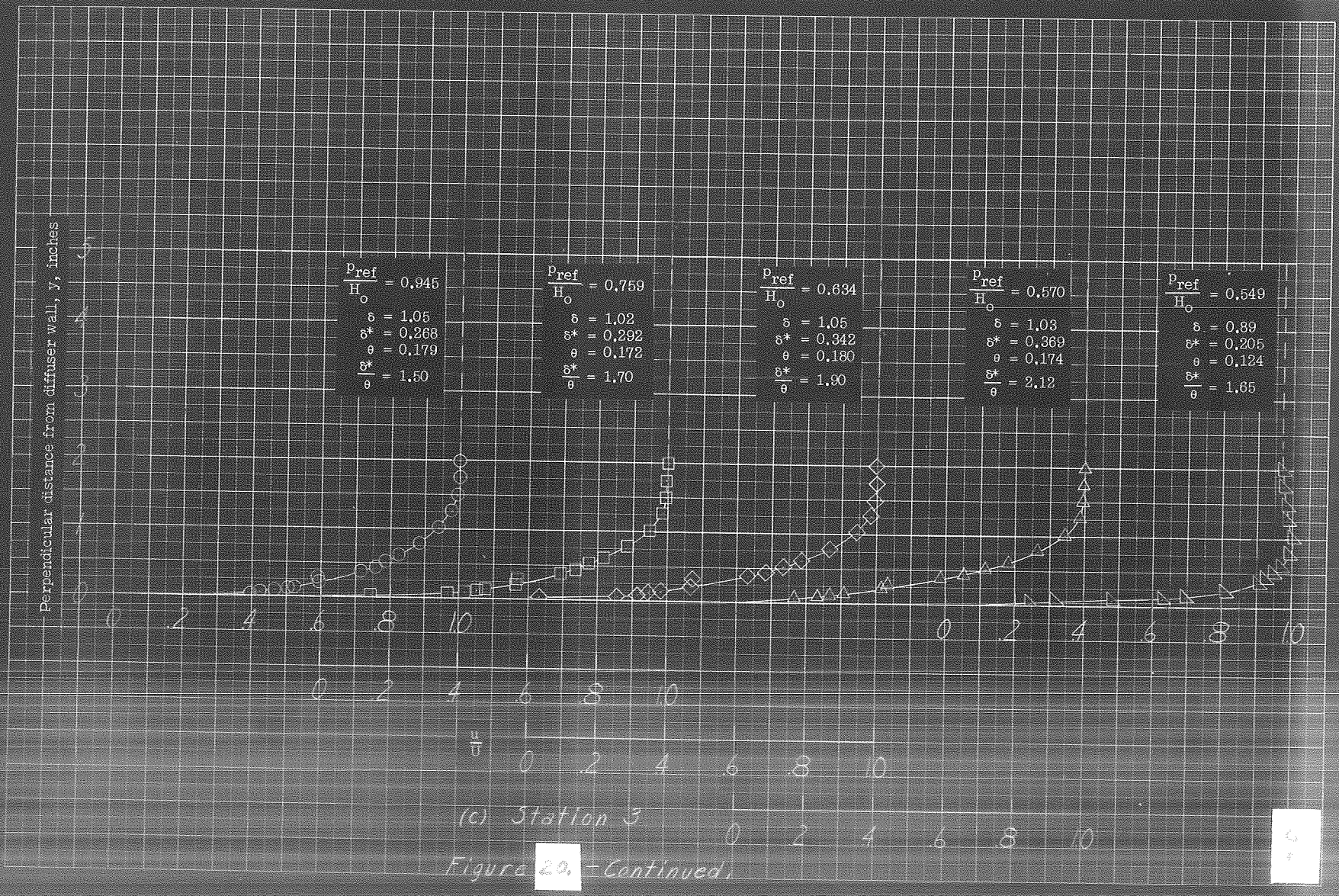

(c) Station 3

Figure 23. - Continued.

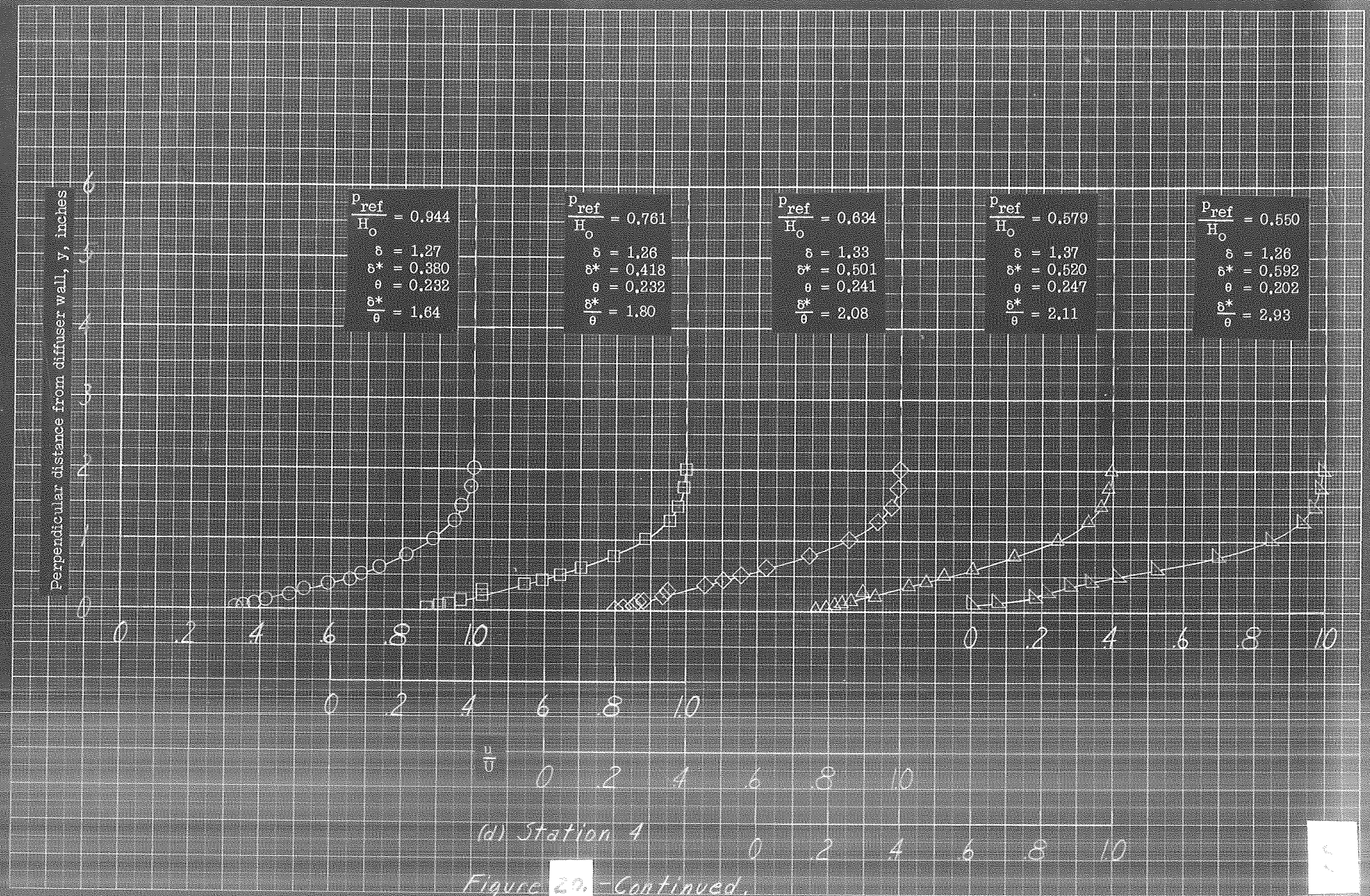

(d) Station 4

Figure 20. -Continued.

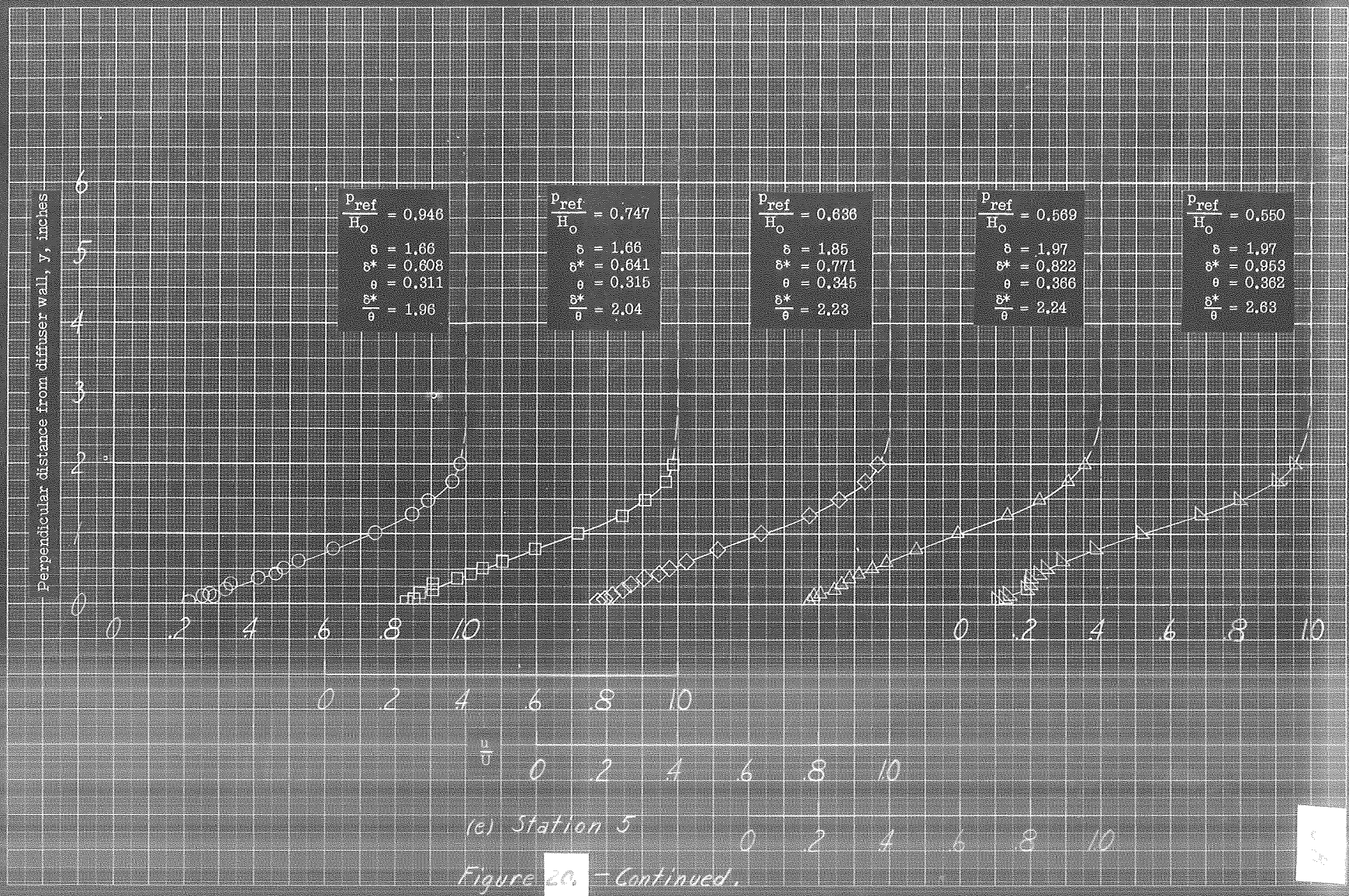

(c) Station 5

Figure 20 – Continued.

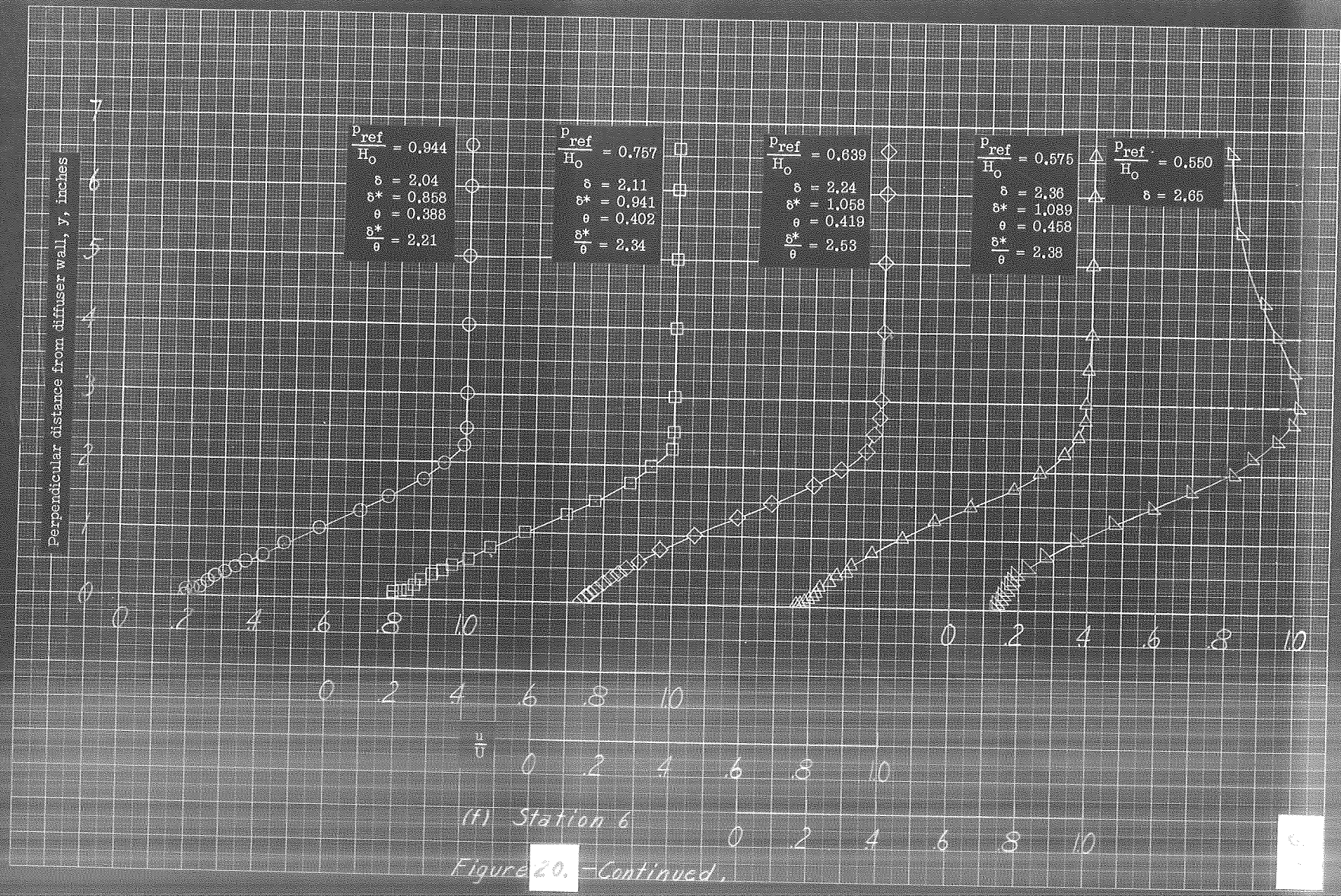

(f) Station 6

Figure 20. – Continued.

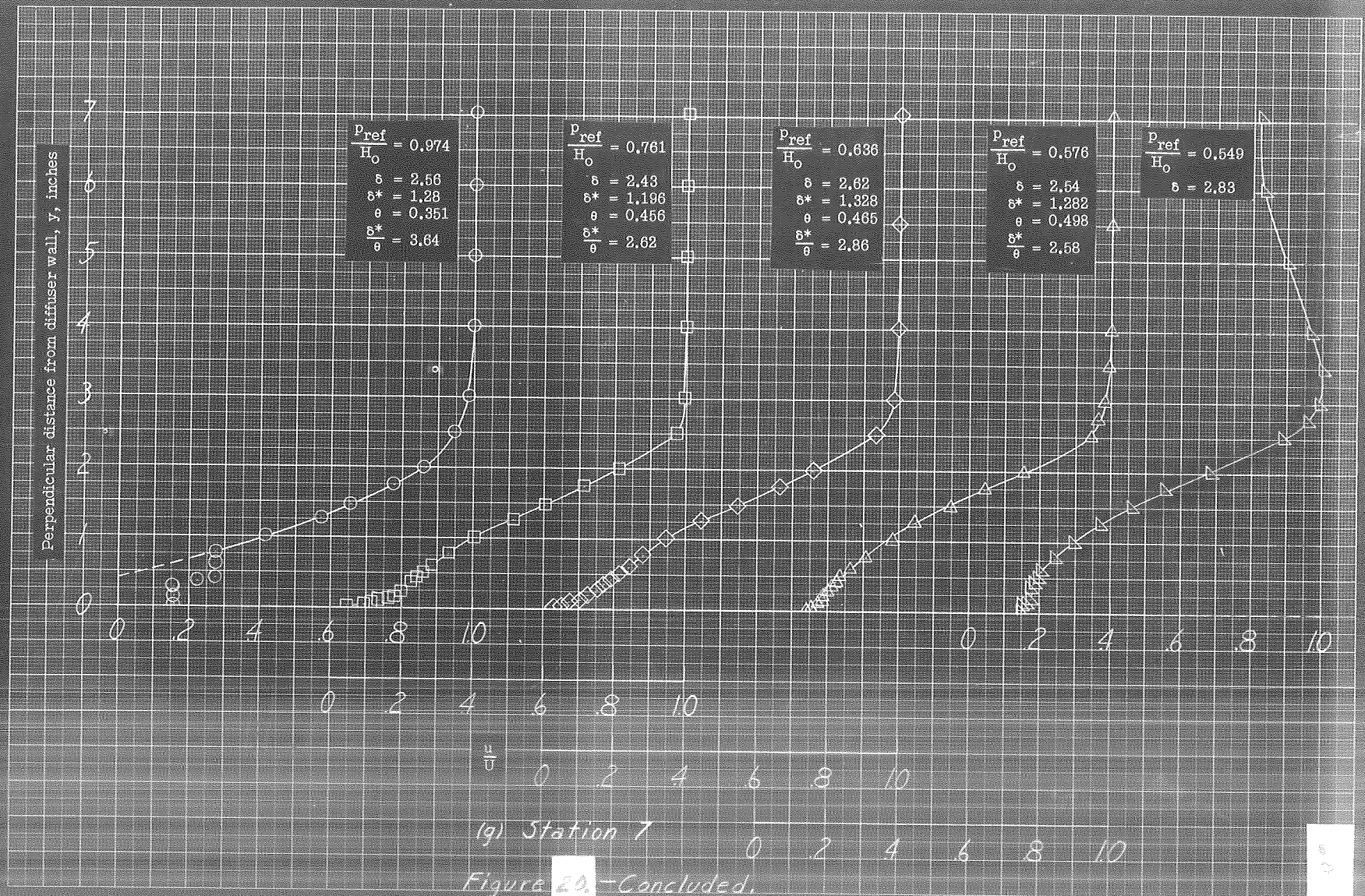

(g) Station 7

Figure 20.—Concluded.

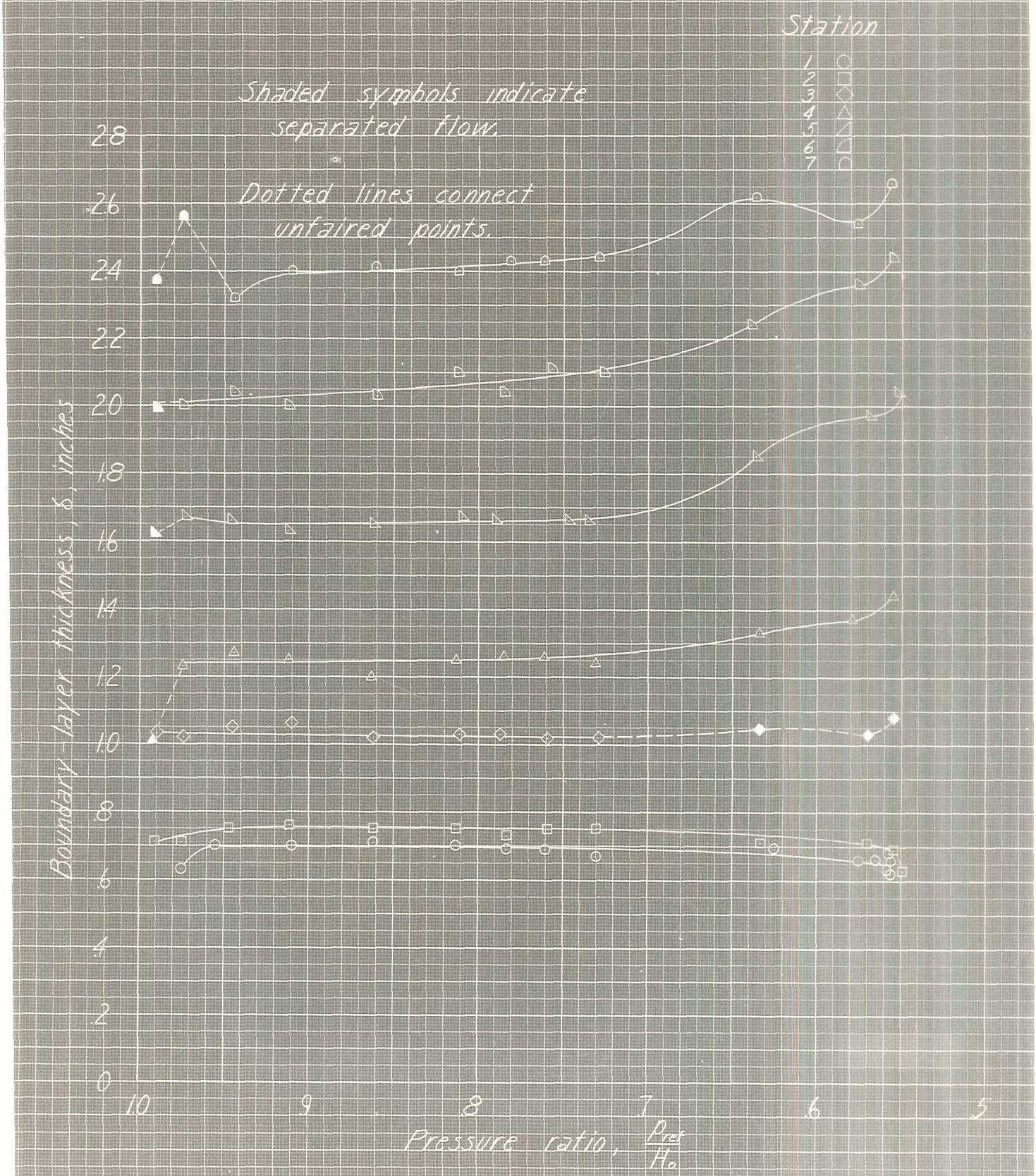

Figure 21. – Variation of boundary-layer thickness with pressure ratio – thicker inlet boundary layer.

KEUFFEL & ESSER CO.
TRADE STANDARD

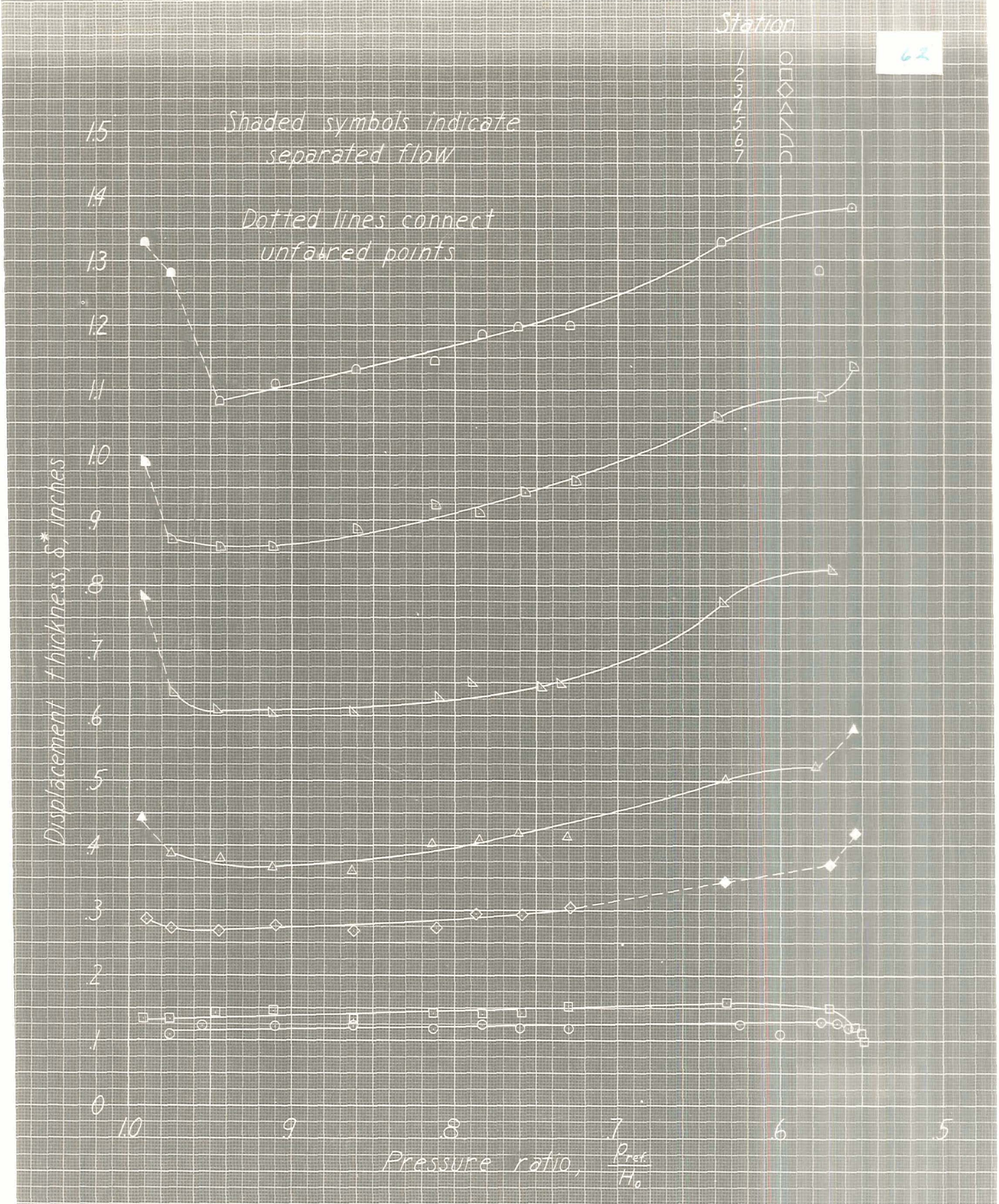

Figure 22. – Variation of displacement thickness with pressure ratio – thicker inlet boundary layer.

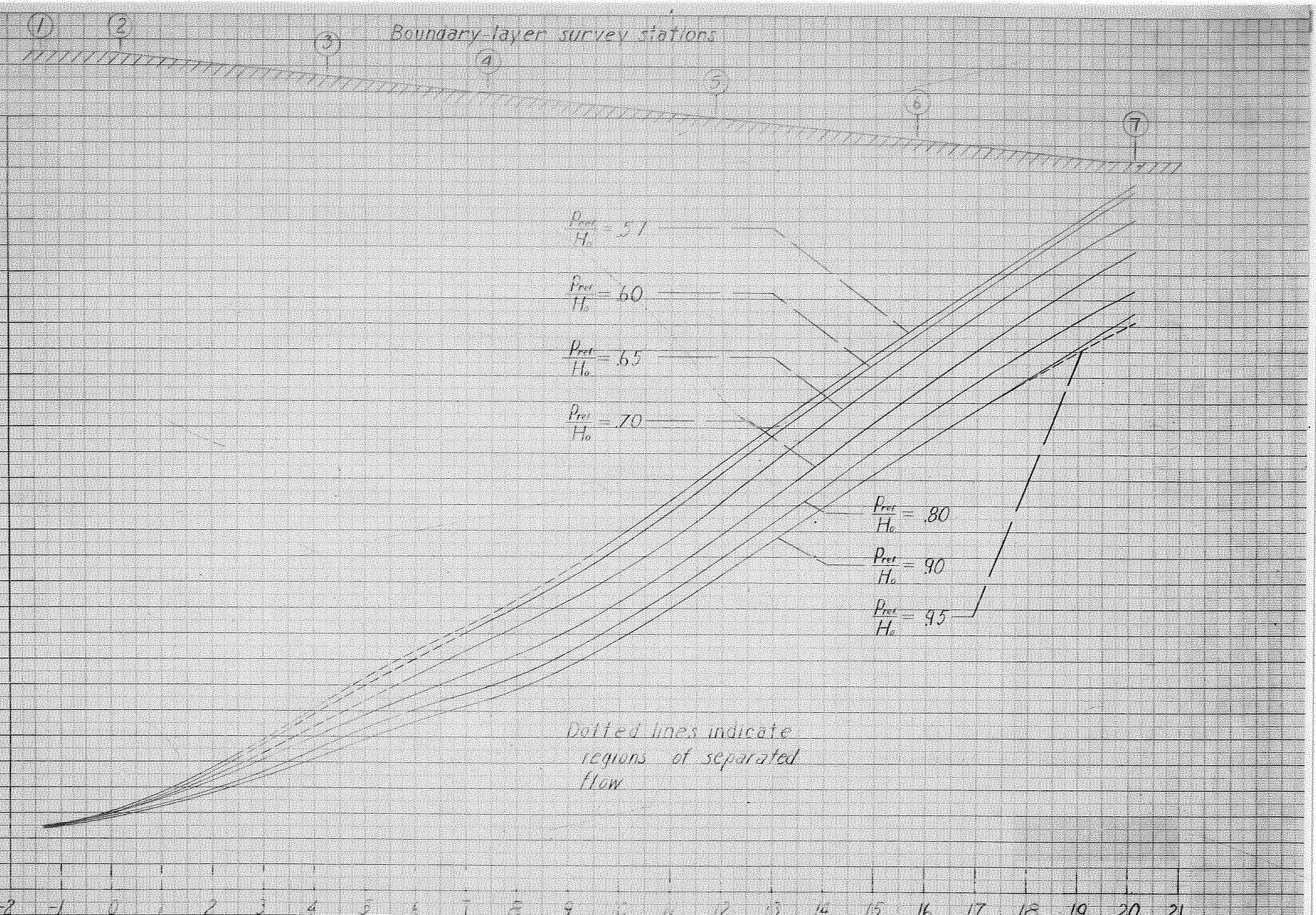

Figure 23. Growth of displacement thickness in the thicker-inlet boundary-layer diffuser.

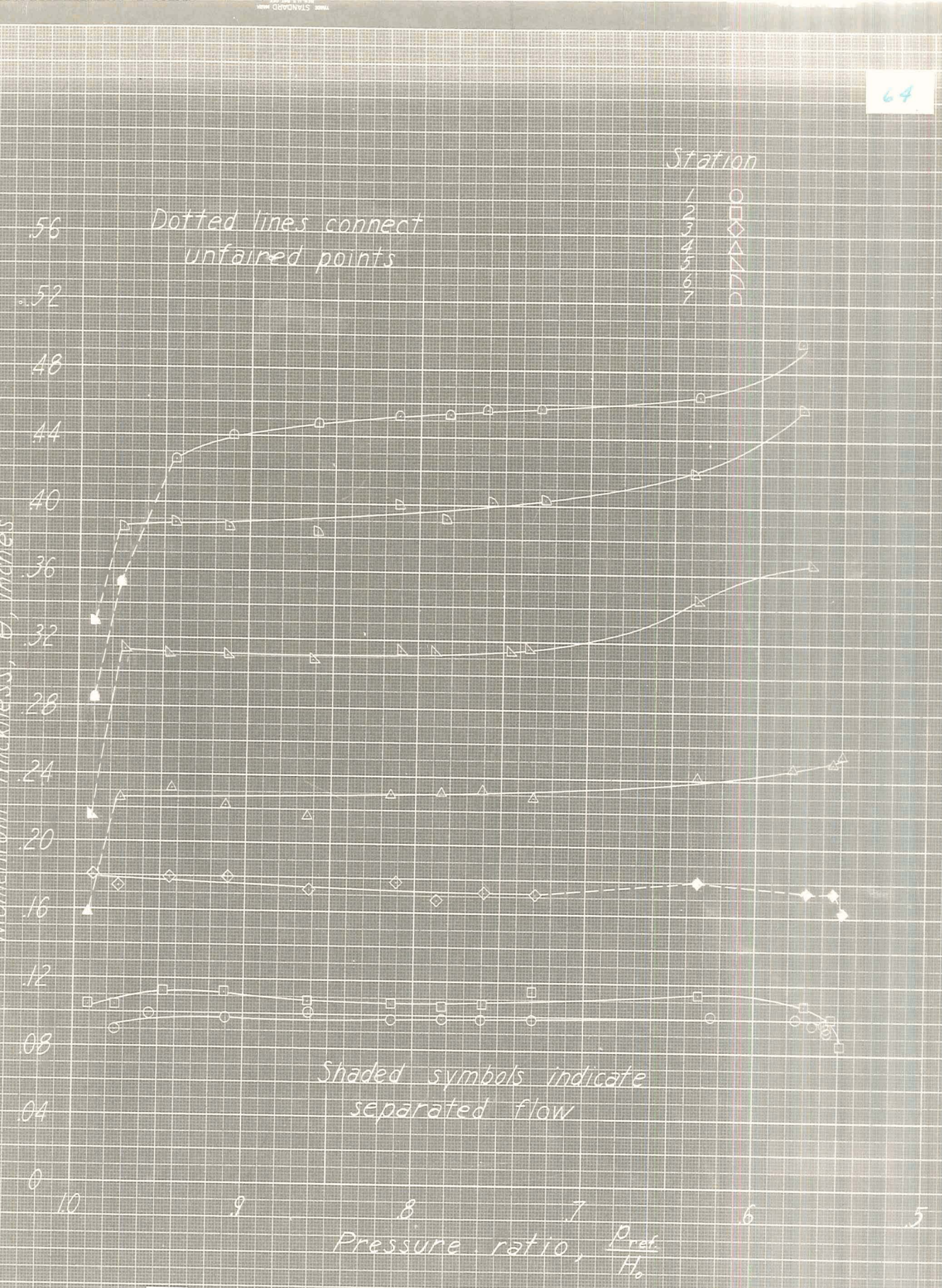

Figure 24. - Variation of momentum thickness with pressure ratio - thicker inlet boundary layer.

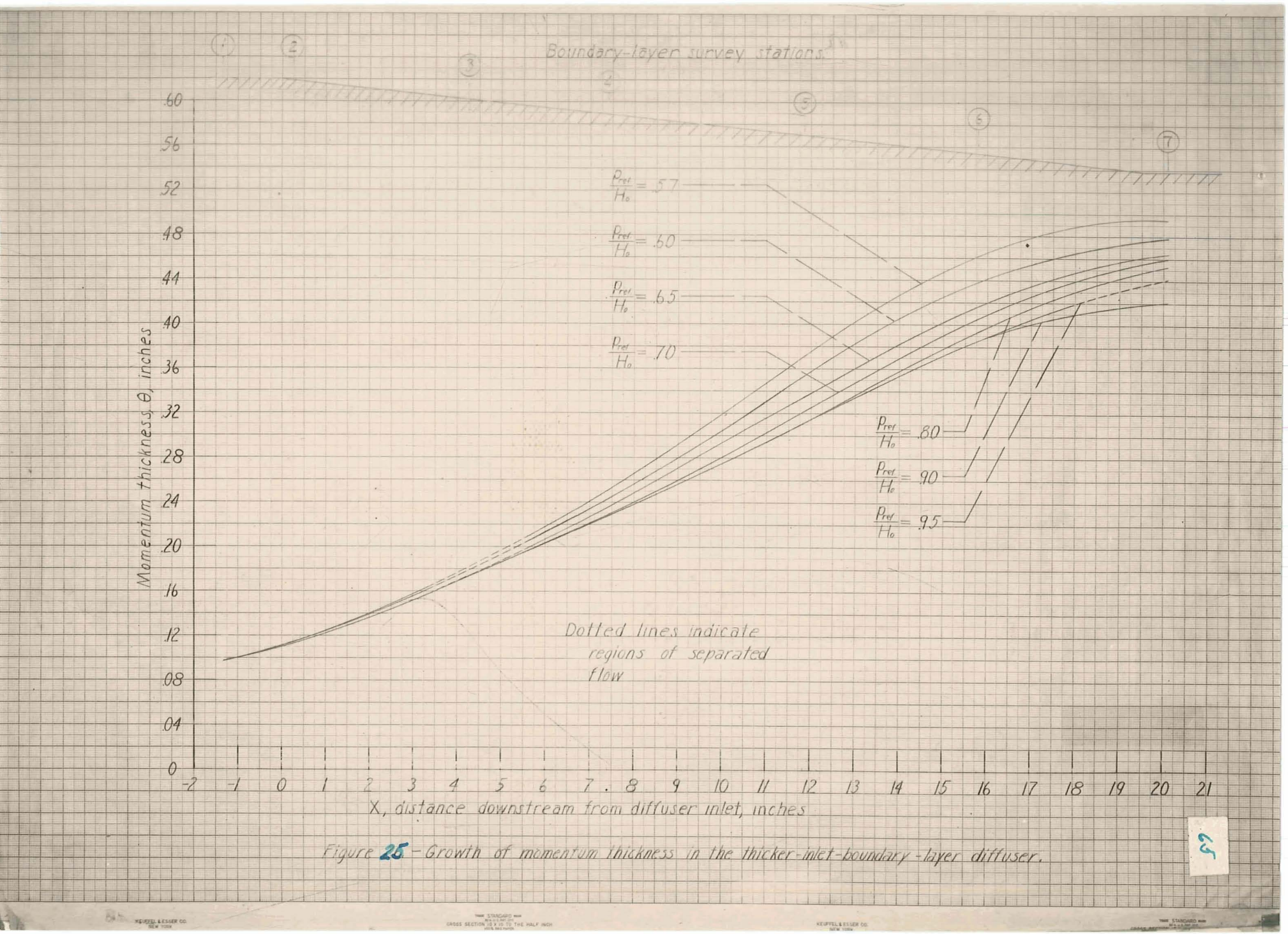

Figure 25 - Growth of momentum thickness in the thicker-inlet-boundary-layer diffuser.

Shaded symbols indicate separated flow

Dotted lines connect unfaired points

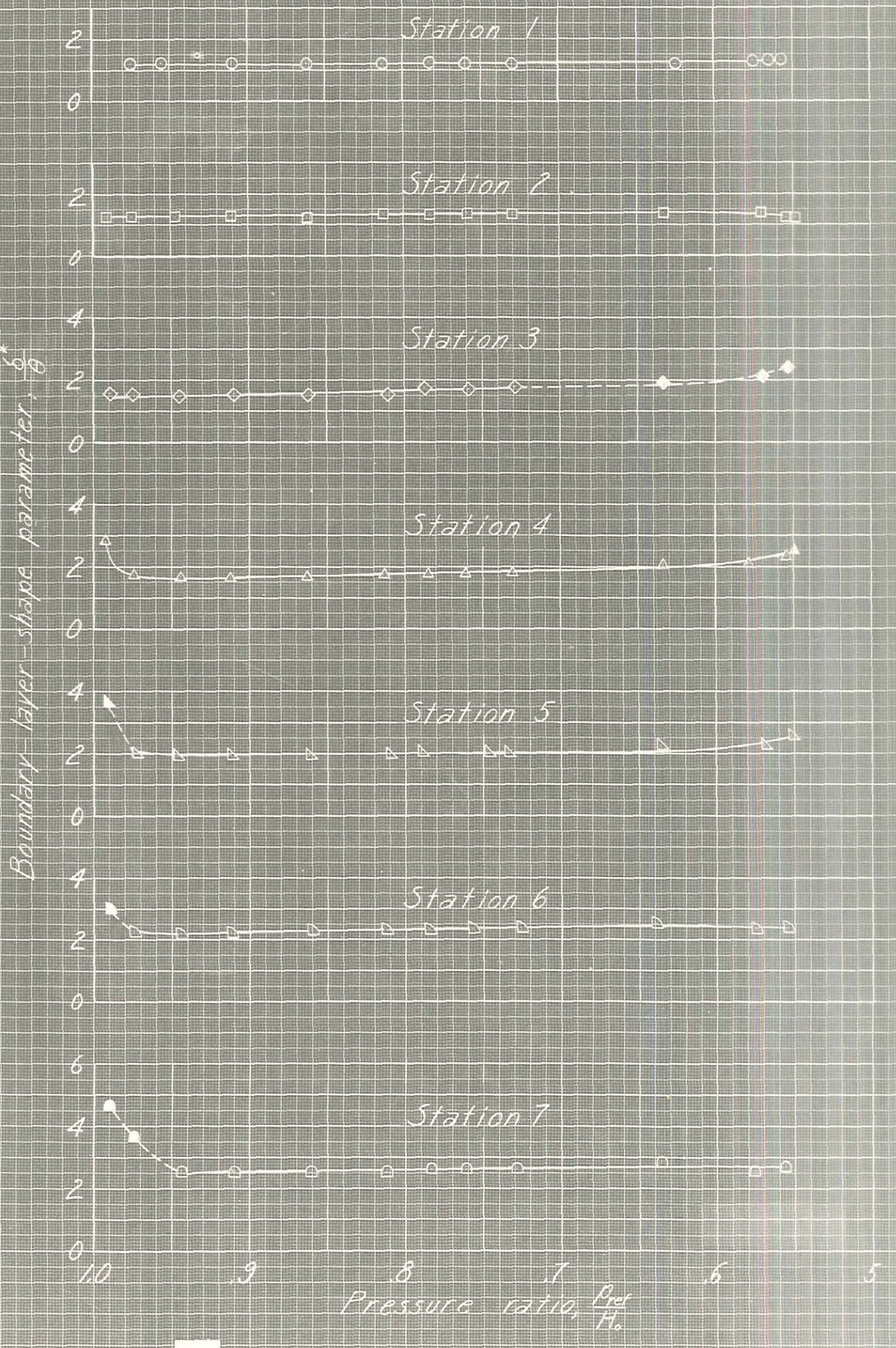

Figure 26. - Variation of boundary-layer-shape parameter with pressure ratio - thicker inlet boundary layer.

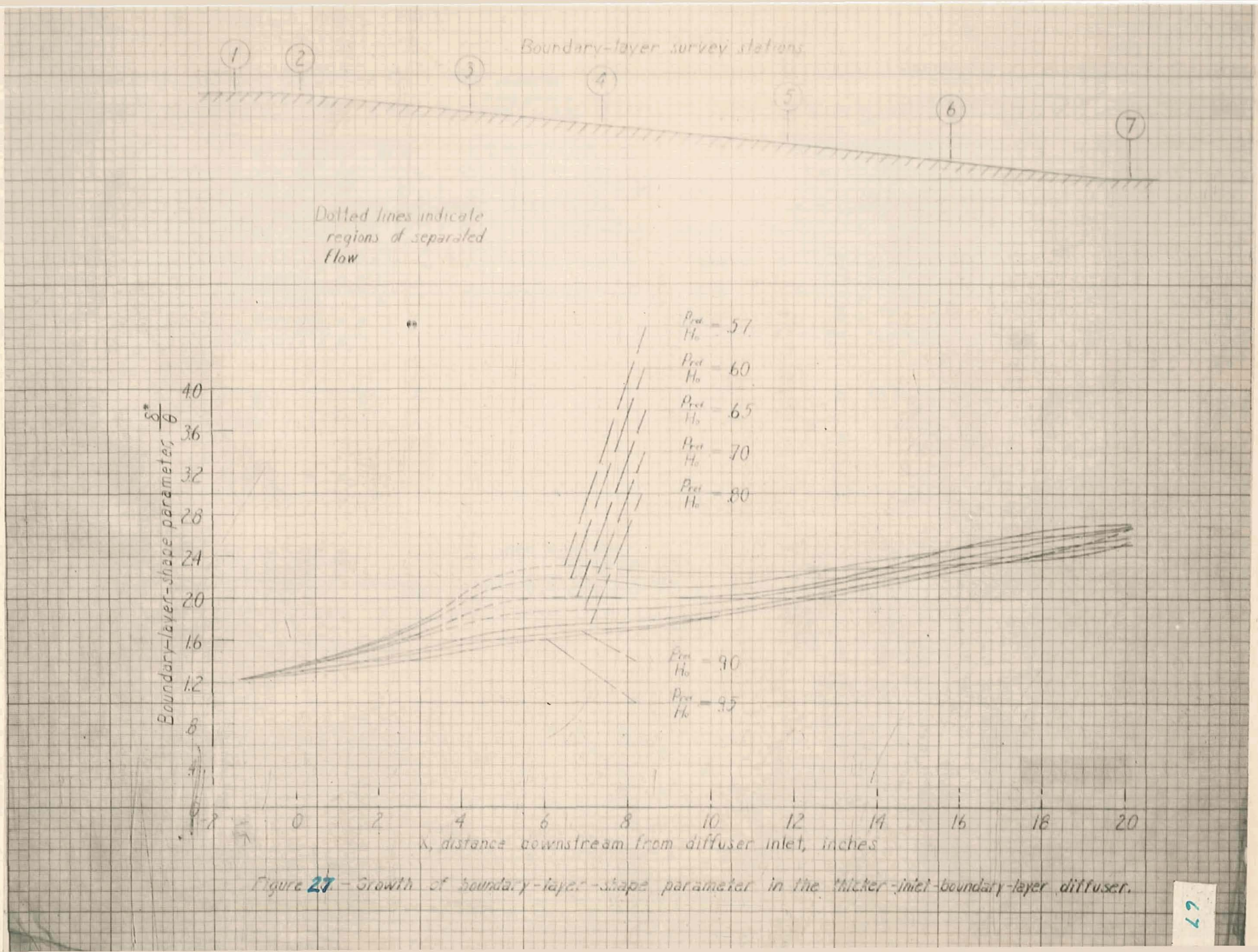

Figure 27 - Growth of boundary-layer-shape parameter in the thicker-inlet-boundary-layer diffuser.

III. COMPARISON OF BOUNDARY LAYERS IN THE TWO CONFIGURATIONS

Boundary-layer profiles at station 1 for the thinner- and the thicker-inlet-boundary-layer configurations are plotted nondimensionally in figure 28. This plot offers a good comparison of the two inlet-boundary-layer conditions. This comparison shows that, in the case of the thicker inlet boundary layer, where a more fully developed turbulent profile appears, more energy is available in the region of low values of $\frac{y}{\delta_1}$ than in the case of the thinner inlet boundary layer. Thus it appears that the thicker-inlet-boundary-layer flow should offer more resistance to separation than the thinner-inlet-boundary-layer flow. This observation is borne out by a re-examination of figures 19 and 27 where the regions of separated flow are shown for the two conditions. These figures show that the thicker inlet boundary layer resists separation better than the thinner inlet boundary layer at all except the lowest flow rates.

Another comparison of the effects of inlet boundary layer on the flow pattern in the diffuser is shown in figure 29. Here the boundary-layer thickness δ and the boundary-layer displacement thickness δ^* are shown schematically for a mean inlet Mach number of about 0.7. The plot of δ shows approximately what part of the geometric area is occupied by boundary layer but no quantitative conclusions can be drawn from this plot. The plot of δ^*, however, gives an indication of what the effective flow expansion in the diffuser actually is. By applying a correction factor to obtain the equivalent three-dimensional δ^* and

using the results to get an effective inlet-to-exit area ratio the diffusion factor $\frac{\Delta q}{\Delta q_{ideal}}$ may be computed so that a quantitative value is obtained. Results obtained from a calculation of this type checked the measured $\frac{\Delta q}{\Delta q_{ideal}}$ values very closely. An example of such an analysis is given in the Appendix.

There are two regions in the diffuser where the action of $\frac{\delta^*}{\theta}$ is notably different in the two configurations. At station 3 for the thicker-inlet-boundary-layer flow (fig. 27) there is no sharp increase in $\frac{\delta^*}{\theta}$ as there is for the thinner-inlet-boundary-layer flow (fig. 19). This is due not only to the more stable entrance velocity profile (fig. 28) but also to the fact that the pressure gradients for the thicker-inlet-boundary-layer flow are not as steep as for the thinner-inlet-boundary-layer flow. In the other region (near station 6) where at the low flow rates for the thinner inlet boundary layer there were high values of $\frac{\delta^*}{\theta}$, the variation of $\frac{\delta^*}{\theta}$ with x for the thicker inlet boundary layer is comparatively steady. It appears that the transfer of energy from the central high-energy flow core into the boundary layer is more nearly sufficient to maintain flow in the thicker boundary layer than in the case of the thinner boundary layer at the flow rates investigated.

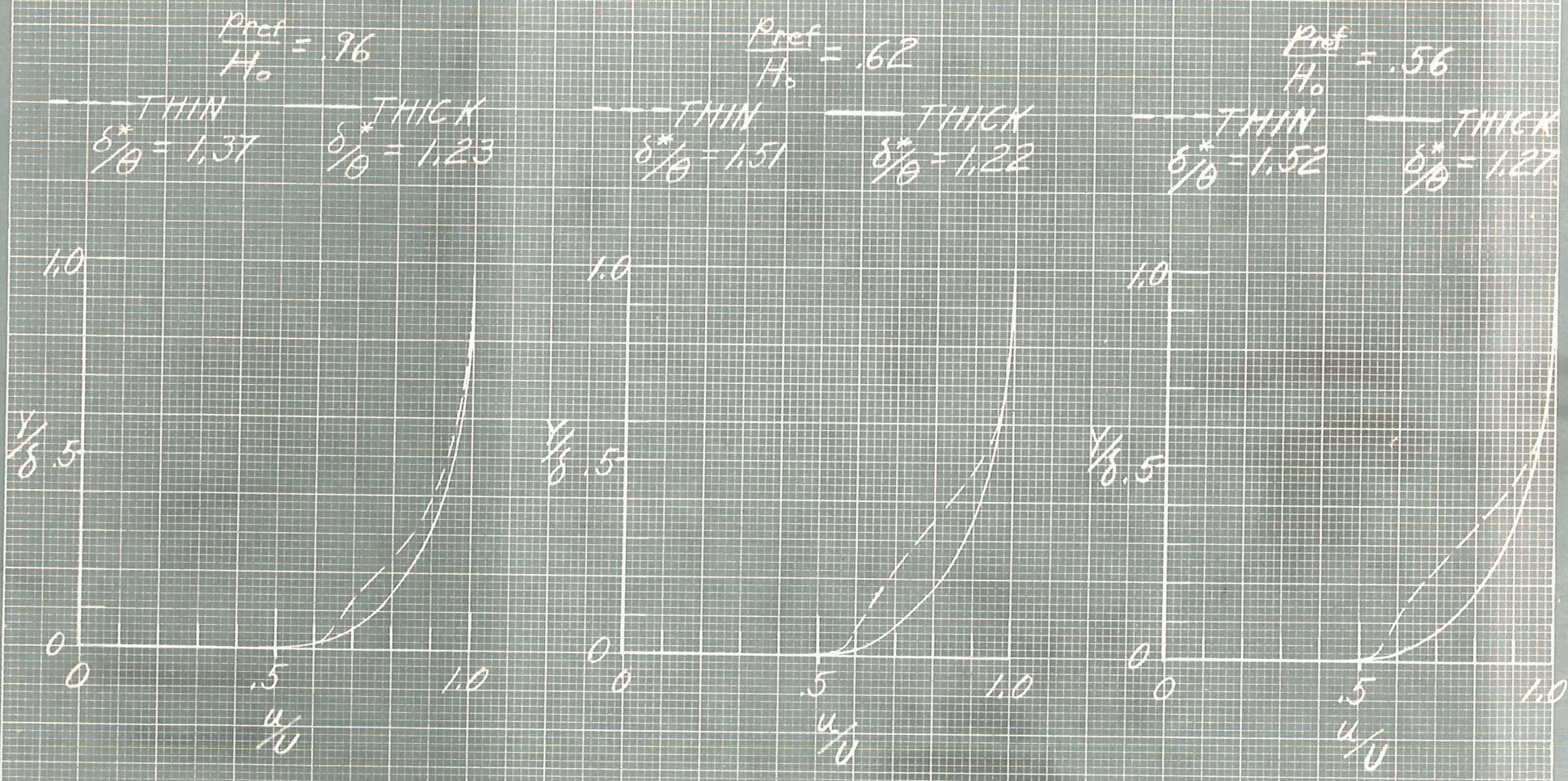

Figure 28. — Comparison of nondimensional velocity profiles at boundary-layer station 1.

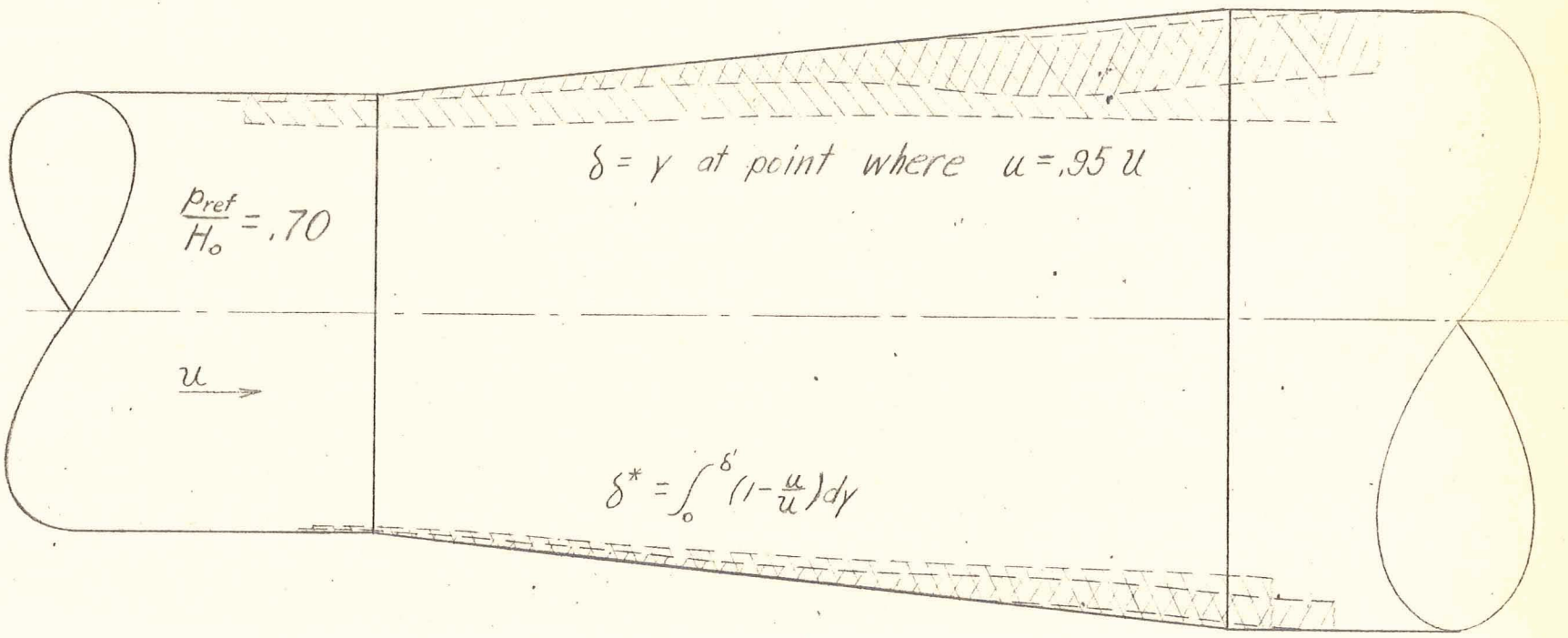

Figure 29. - Comparison of boundary layer thickness parameters δ and δ^* in the diffuser.

CHAPTER VIII

RESULTS OF PERFORMANCE MEASUREMENTS AND DISCUSSION

The value of a diffuser is measured in terms of total pressure loss and static-pressure rise, regardless of what pattern the flow takes. By examining performance in terms of several parameters, however, it can be shown just what effect different phases of the flow pattern have, and consequently a better idea of what can be done to improve performance may be obtained.

I. LOSS COEFFICIENT

The loss coefficient $\frac{\Delta H}{q_i}$ is plotted against $\frac{p_{ref}}{H_o}$ for both the thinner and thicker inlet boundary layers in figure 30. Since a boundary layer is inherently a region of energy or pressure loss, it should be expected that the loss coefficient be higher for the thicker-boundary-layer flow.

For the thinner inlet boundary layer $\frac{\Delta H}{q_i}$ is practically constant at 0.025 through most of the subsonic range. This parameter increases slightly in the high-subsonic range but does not increase appreciably until the pressure losses created by local supersonic flow and consequent shock waves occur at $\frac{p_{ref}}{H_o}$ values less than 0.6. These shock losses increase in intensity as the system chokes and the maximum Mach number becomes greater.

For the thicker inlet boundary layer $\frac{\Delta H}{q_i} = 0.055$ through most of the low-subsonic range. In the range $M > 0.7$ $\left(\frac{p_{ref}}{H_o} \approx 0.7\right)$ $\frac{\Delta H}{q_i}$

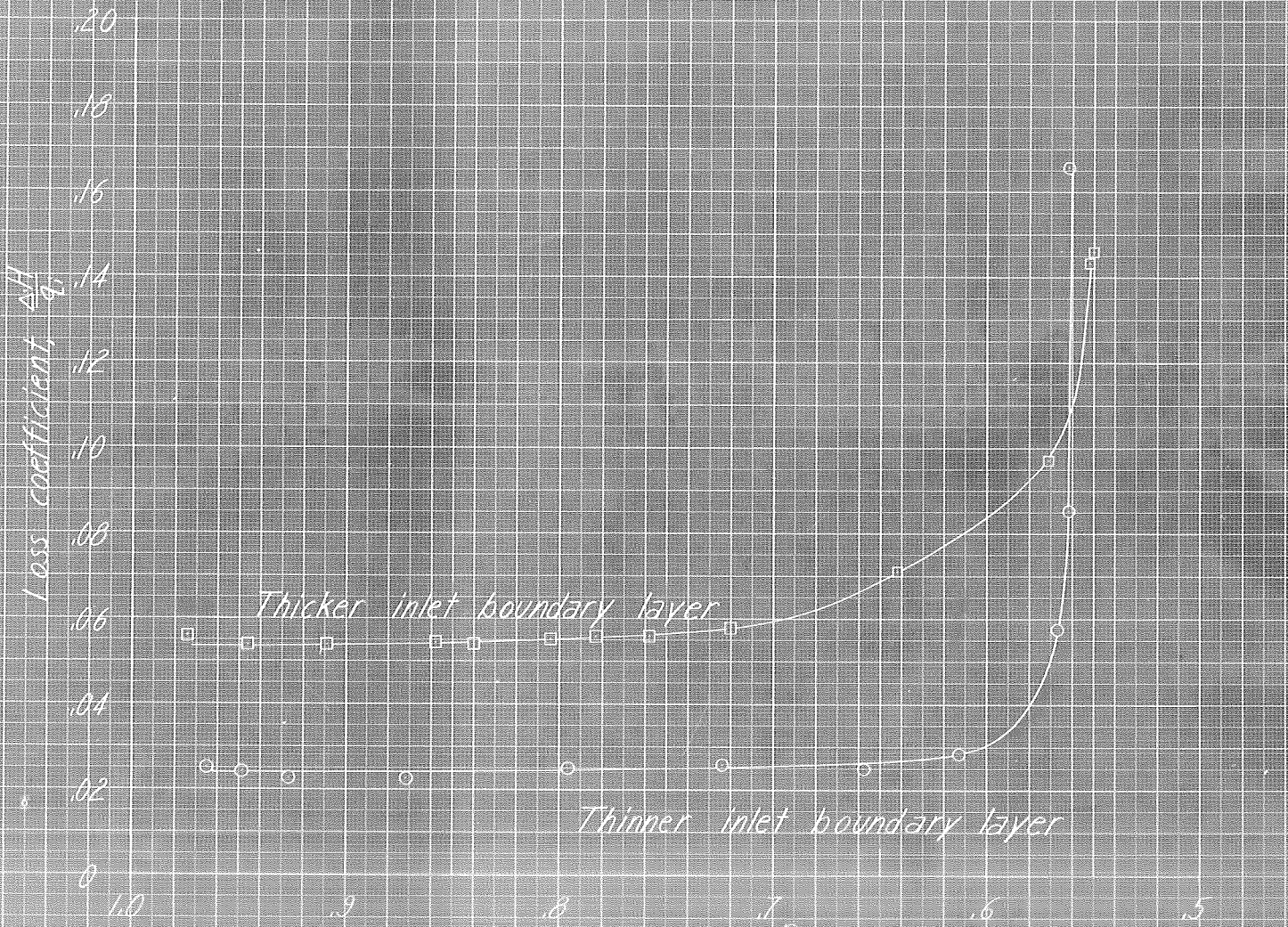

Figure 30. - Variation of loss coefficient with pressure ratio.

increases more rapidly with increasing flow rate than in the case of the thinner inlet boundary layer. In this range also, increases in the displacement thickness and momentum thickness become more pronounced as shown in figures 22 and 24, respectively. Local regions of supersonic flow appear at about $\frac{P_{ref}}{H_o} = 0.56$ and here the pressure losses as measured by $\frac{\Delta H}{q_1}$ increase sharply.

II. DIFFUSION FACTOR

The diffusion factor $\frac{\Delta q}{\Delta q_{ideal}}$ is plotted in figure 31. This parameter measures how much of the possible geometric expansion is actually utilized. For the thinner boundary layer the presence of separation at the diffuser exit at all flow rates makes the values of $\frac{\Delta q}{\Delta q_{ideal}}$ lower than would be expected, but the thicker-boundary-layer flow, even with less separation, produces even lower values. In the low-subsonic-flow range, for the thinner boundary layer $\frac{\Delta q}{\Delta q_{ideal}} \approx 0.86$, and for the thicker inlet boundary layer $\frac{\Delta q}{\Delta q_{ideal}} \approx 0.73$.

Comparison of these values with those of reference 8, in which a similar investigation was carried out in a 21-inch-diameter diffuser, shows that for both boundary-layer conditions the values of $\frac{\Delta q}{\Delta q_{ideal}}$ for the 10-inch diffuser are about 0.10 lower than those for the larger diffuser. This difference can be explained if the ratio of $\left(\frac{\delta^*}{\text{Diameter}}\right)_i$ is examined, for such examination shows that $\left(\frac{\delta^*}{\text{Diameter}}\right)_i$ for the smaller diffuser is of the order of twice as large as for the larger diffuser, or in other words, the smaller diffuser has less geometric

Figure 31. Variation of diffusion factor with pressure ratio.

efficiency than the larger diffuser.

With increasing flow rate $\frac{\Delta q}{\Delta q_{ideal}}$ decreases slightly in both thinner- and thicker-boundary-layer configurations because of increasing rate of growth of boundary layer and increasing severity of flow separation.

III. PRESSURE EFFICIENCY

The pressure efficiency $\frac{\Delta p}{\Delta q}$ is plotted in figure 32. This parameter, since it measures the ability of the diffuser to convert the change in dynamic pressure through the diffuser to static pressure, will be largely dependent upon pressure losses through the system and can therefore be expected to vary similarly to $\frac{\Delta H}{q_i}$. It can be seen that for the thinner-boundary-layer flow $\frac{\Delta p}{\Delta q}$ is practically constant at about 0.96 until shock losses cause the sharp decrease at $\frac{p_{ref}}{H_o} < 0.57$ where regions of local supersonic flow are attained. For the thicker-boundary-layer flow $\frac{\Delta p}{\Delta q}$ is practically constant over the lower subsonic range at about 0.90 but in the higher subsonic range the values decrease more rapidly with increasing flow rate than was the case for the thinner-boundary-layer flow.

IV. DIFFUSER EFFECTIVENESS

The diffuser effectiveness $\frac{\Delta p}{\Delta p_{ideal}}$ is plotted against $\frac{p_{ref}}{H_o}$ in figure 33. Since the over-all diffuser effectiveness $\frac{\Delta p}{\Delta p_{ideal}}$ is

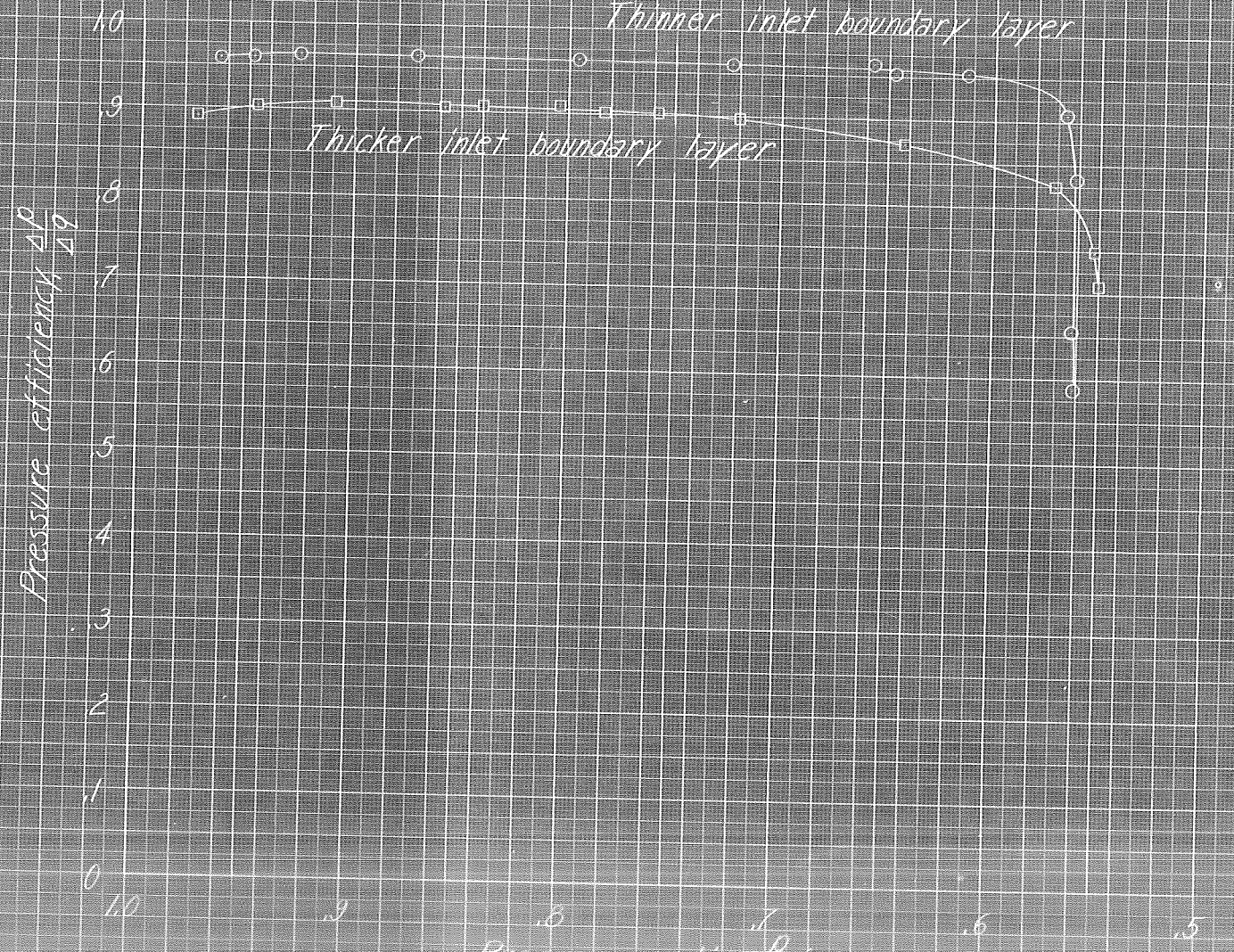

Figure 32.- Variation of pressure efficiency with pressure ratio.

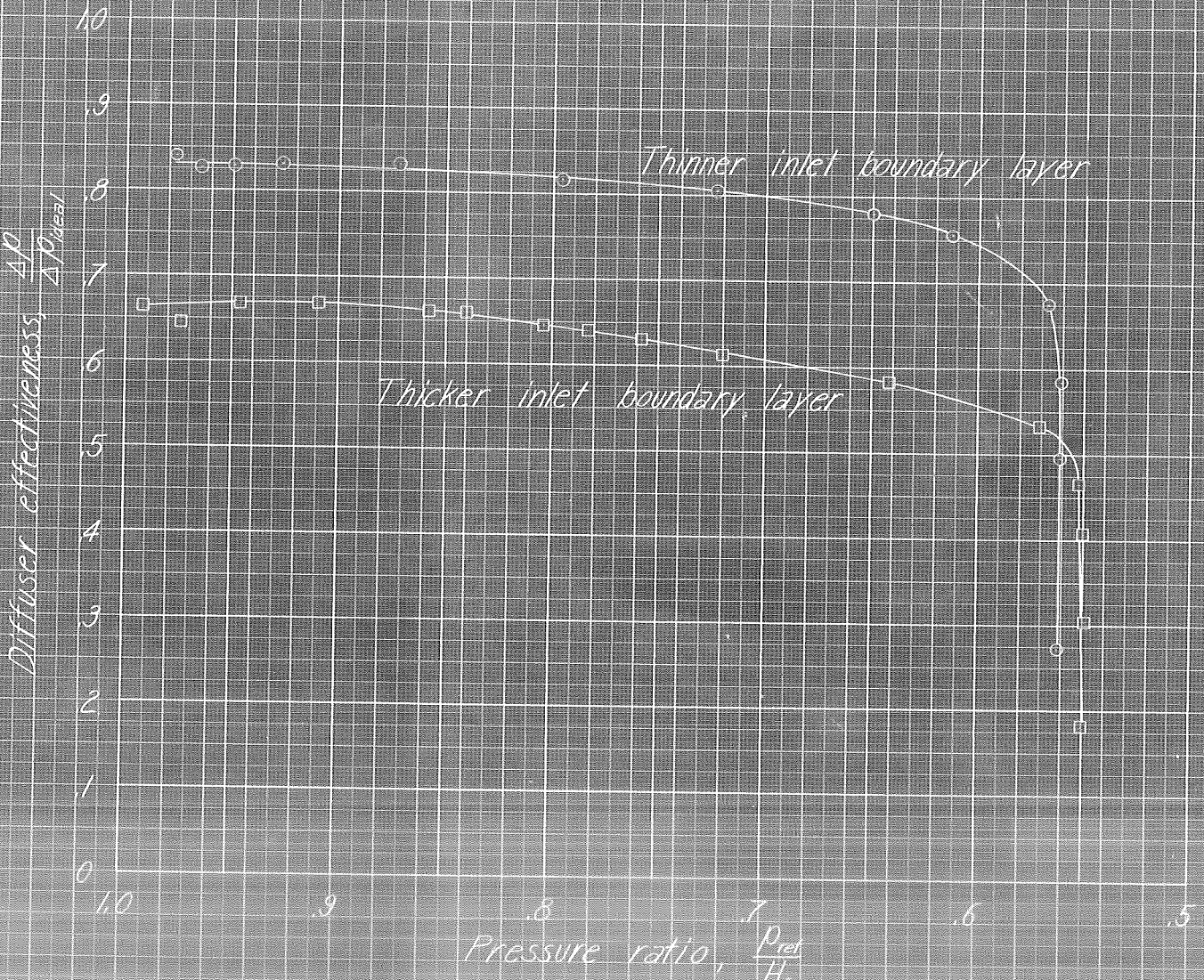

Figure 33. - Variation of diffuser effectiveness with pressure ratio.

the product of the diffusion factor $\frac{\Delta q}{\Delta q_{ideal}}$ and the pressure efficiency $\frac{\Delta p}{\Delta q}$, its behavior is explained by the action of these two parameters. For the thinner-boundary-layer flow $\frac{\Delta p}{\Delta p_{ideal}}$ is constant at about 0.82 in the lower subsonic flow range and decreases slowly with increasing flow rate until the diffuser chokes, at which point the values drop rapidly. For the thicker-boundary-layer flow $\frac{\Delta p}{\Delta p_{ideal}}$ is about 0.67 at low flow rates and the curve behaves in a manner similar to that of the thinner inlet boundary layer.

Throughout the subsonic flow range the performance of the thinner-boundary-layer configuration is better in every respect than the thicker-boundary-layer configuration. The primary reason for this is shown to be not so much the increased pressure loss inherent in a thicker boundary layer but rather the decrease in effective expansion ratio as represented by the parameter $\frac{\Delta q}{\Delta q_{ideal}}$.

CHAPTER IX

SUMMARY AND CONCLUSIONS

From the results of this investigation and their analysis it is now possible to summarize what has been done and to draw some conclusions as to the significance of these findings.

I. SUMMARY

Flow conditions and performance parameters were studied in a 12° 10-inch-inlet-diameter conical diffuser of 2:1 exit-to-inlet area ratio under two inlet-boundary-layer conditions. Two lengths of constant-area inlet pipe were used ahead of the diffuser entrance - one 9-inches long and the other 68-inches long. These different lengths of inlet pipe produced two inlet boundary layers characterized by displacement thicknesses of about 0.034 inch and 0.120 inch, respectively.

Investigations of static-pressure distributions, boundary-layer profiles and shape parameters, and performance parameters were made and their actions and reactions upon one another were studied over a wide range of flow rates. The flow rate was varied by increasing total pressure upstream of the diffuser system so that mean inlet Mach number was varied from about 0.20 to 0.84 and mean inlet Reynolds number was varied from about 1.0×10^6 to 4.0×10^6.

It was found that the thicker-inlet-boundary-layer flow pattern was much more stable than the thinner-inlet-boundary-layer flow pattern;

i.e., it resisted the tendency to separate from the wall better. But in spite of this the over-all efficiency of the thinner-inlet-boundary-layer configuration was about 15 percent higher because primarily more of the available expansion area was available for use in converting dynamic pressure to static pressure, and secondarily because the pressure losses in the thinner boundary layer were less.

II. CONCLUSIONS

From the results of this investigation the following conclusions are drawn:

(1) The inlet-boundary-layer profile is an important variable in the performance of a diffuser.

(2) For the two conditions investigated the performance, measured as the ratio of actual static-pressure increase through the diffuser to the static pressure increase ideally possible, varied inversely with increasing inlet-boundary-layer thickness.

(3) Diffuser effectiveness for both inlet-boundary-layer conditions is reduced more by failure to realize the theoretically possible change in dynamic pressure than by losses incurred in converting the available change in dynamic pressure to a change in static pressure. This is caused by the action of the boundary layer in reducing the effective expansion of the diffuser geometry.

(4) From the preceding conclusion it follows that the diffuser efficiency would most effectively be increased through some

method whereby boundary-layer growth might be reduced to a minimum and the separation of the flow from the wall be eliminated. This might involve boundary-layer control by means of continuous suction through porous walls or the removal of low energy air near the wall through slots placed at points where strong adverse pressure gradients create rapid boundary-layer growth.

BIBLIOGRAPHY

REFERENCES

1. von Doenhoff, Albert E., and Tetervin, Neal: Determination of General Relations for the Behaviour of Turbulent Boundary Layers. NACA Report 772, 1943.
2. Gibson, A. H.: On the Flow of Water through Pipes and Passages Having Converging or Diverging Boundaries. Proc. Roy. Soc. (London), Ser. A, Vol. 83, No. 563, March 2, 1910, pp. 366-378.
3. Squire, H. B.: Experiments on Conical Diffusers. Report No. Aero. 2216, British R.A.E., August 1947.
4. Bohm, H., and Koppe, M.: The Influence of Friction on Steady Diffuser Flows at High Speed. Joint Intelligence Objectives Agency (Washington), July 23, 1946.
5. Naumann: Wirkungsgrad von Diffusoren bei hohen Unterschallgeschwindigkeiten. FB Nr. 1705, Deutsche Luftfahrtforschung (Berlin-Adlershof), 1942.
6. Peters, H.: Conversion of Energy in Cross-Sectional Divergencies under Different Conditions of Inflow. NACA TM 737, 1934.
7. Patterson, G. N.: Modern Diffuser Design. Aircraft Engineering, Vol. X, No. 115, Sept. 1938, pp. 267-273.
8. Henry, John R.: Design of Power-Plant Installations. Pressure Loss Characteristics of Duct Components. NACA ARR L4F26, 1944.
9. Persh, Jerome: The Effect of the Inlet Mach Number and Inlet-Boundary-Layer Thickness on the Performance of a 23° Conical Diffuser Tail-Pipe Combination. NACA RM L9K10, 1950.

10. Copp, Martin R., and Klevatt, Paul L.: Investigation of High-Subsonic Performance Characteristics of a 12° 21-Inch Conical Diffuser, Including the Effects of Change in Inlet-Boundary-Layer Thickness. NACA RM L9H10, 1950.

APPENDIX

COMPARISON OF MEASURED VALUES OF $\frac{\Delta q}{\Delta q_{ideal}}$ WITH THOSE CALCULATED FROM THE BOUNDARY-LAYER DISPLACEMENT THICKNESS

Since δ^* is small relative to the diameter of the duct it may be assumed that the two-dimensional value of δ^* used in this investigation is approximately the true δ^*. If then it is assumed that the displacement thickness is a measure of the amount that the boundary layer effectively displaces the flow streamlines from the wall, the effective diameter at the diffuser exit is

$$(D_e)_{effective} = D_e - 2\delta^*$$

The values measured for δ^* at the exit station for a mean inlet Mach number of about 0.7 $\left(\frac{P_{ref}}{H_o} = 0.7\right)$ are 0.75 inch for the thinner-inlet-boundary-layer condition.

Then

$$(D_e)_{effective} = 14.14 - 2 \times 0.75$$
$$= 12.64 \text{ inches}$$

For a rough approximation the equation $\Delta q = q_i \left[1 - \left(\frac{A_i}{A_e}\right)^2\right]$ may be used (assuming incompressible flow).

Then for the thinner-boundary-layer case

$$\Delta q = q_i \left[1 - \left(\frac{10}{12.64}\right)^4\right],$$
$$= q_i \ (1 - 0.39),$$
$$= 0.61 \ q_i$$

If there were no boundary layer

$$\Delta q_{ideal} = q_i \left[1 - \left(\frac{10}{14.14}\right)^2\right]$$

$$= q_i \ (1 - 0.25)$$

$$= 0.75 \ q_i$$

So the diffusion factor $\frac{\Delta q}{\Delta q_{ideal}}$ is

$$\frac{\Delta q}{\Delta q_{ideal}} = \frac{0.61}{0.75} = 0.82$$

The value calculated from actual pressure measurement is

$$\frac{\Delta q}{\Delta q_{ideal}} = 0.84 \text{ (thinner boundary layer)}$$

Considering the many simplifying assumptions used in this method of calculation these values compare very well and this rough analysis indicates how the performance parameter $\frac{\Delta q}{\Delta q_{ideal}}$ is directly connected with boundary-layer action.

It should be pointed out, however, that similar analyses in conical diffusers with greater included angles have not resulted in such good agreement. It is believed that this is caused by the inaccuracies involved in measuring velocity profiles in regions of highly turbulent flow.